Coordination Chemistry Reviews
210 (2000) 329–367

COORDINATION
CHEMISTRY
REVIEWS

www.elsevier.com/locate/ccr

# Non-cyclopentadienyl organometallic compounds of calcium, strontium and barium

Timothy P. Hanusa *

*Department of Chemistry, Vanderbilt University, Nashville, TN 37235, USA*

Received 8 October 1999; accepted 2 December 1999

## Contents

---

* Tel.: + 1-615-3222861; fax: + 1-615-3431234.
*E-mail address:* t.hanusa@vanderbilt.edu (T.P. Hanusa)

PII: S0010-8545(00)00348-9

## Abstract

The use of sterically demanding ligands has allowed the organometallic compounds of the heavy alkaline-earth metals calcium, strontium and barium to emerge from the shadow cast by the far better studied organomagnesium Grignard reagents. Metallocenes and other cyclopentadienyl-based complexes have been the most intensively investigated, but in the past decade a wealth of new non-cyclopentadienyl compounds have been characterized. A broad range of structure types are known, encompassing $\sigma$- and $\pi$-bound anionic ligands, and Lewis base adducts with neutral donors. In this review, crystallographically characterized complexes are discussed, and current interpretations of the bonding in heavier Group 2 element compounds are examined. Recent applications of non-cyclopentadienyl compounds in organic synthesis are surveyed.

*Keywords:* Organometallic compounds; Calcium; Strontium; Barium; Non-cyclopentadienyl compounds

## 1. Introduction

Until the mid-1980s, the organic derivatives of calcium, strontium and barium possessed the dual status of being among the longest known yet least understood of any class of organometallic complexes. Only a few years after the arrival of Grignard reagents in 1900, the first reports of analogous compounds of the heavier alkaline-earth metals began to appear [1]. Despite attempts by several researchers, notably H. Gilman and coworkers [2,3], to develop useful synthetic reagents from these metals, expectations that new compounds as valuable as the Grignards might be found went unfulfilled. Almost without exception, the ‘RMX’ derivatives of calcium, strontium, and barium were more difficult to prepare, less thermally stable, and less selective in their reactions than their magnesium counterparts. There were no practical synthetic advantages to justify the complications in using the heavier metals, and research efforts in the area waned.

In the wake of the discovery of ferrocene in 1951 [4], the general interest in metal cyclopentadienyl compounds prompted several groups to attempt the synthesis of alkaline-earth metallocenes. Within a few years, the hydrocarbon-soluble bis(cyclopentadienyl)beryllium (1959) [5] and bis(cyclopentadienyl)magnesium (1955) [6] were made, along with the analogous metallocenes of calcium (1956) [7], strontium (1961) and barium (1961) [8]. Even though they were thermally stable, the yields for the strontium and barium derivatives were extremely low ( $< 5\%$), and none of the base-free $MCp_2$ compounds of the calcium subgroup metals were soluble in common organic solvents such as ethers or hydrocarbons. Their insolubility stemmed from polymeric structures, as demonstrated crystallographically for $CaCp_2$ (Fig. 1) [9].

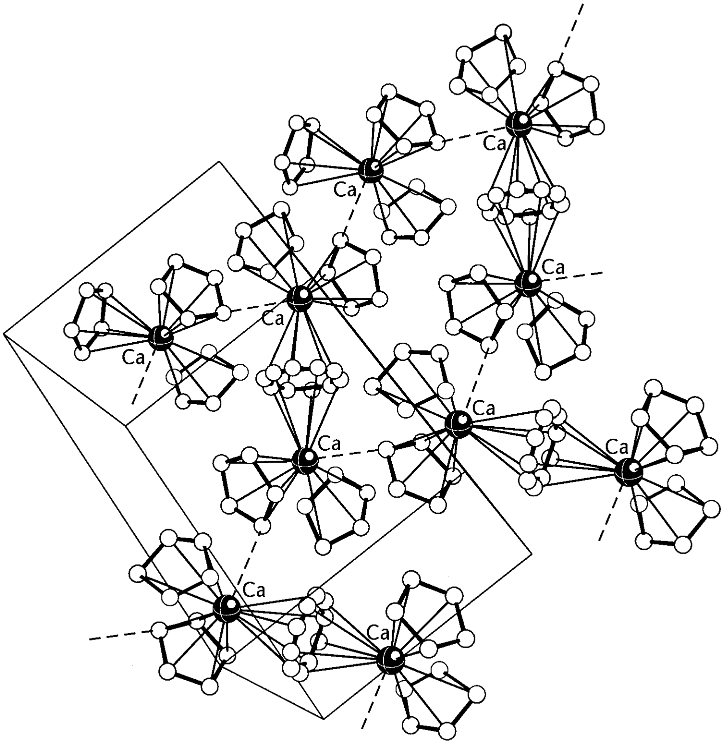

Fig. 1. Packing diagram of $CaCp_2$ [9], illustrating the ‘chains’ of $CaCp_2$ units ‘crosslinked’ with disordered cyclopentadienyl rings.

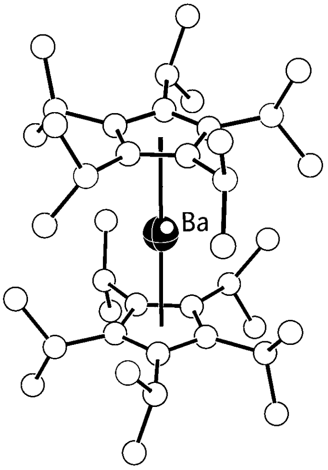

Fig. 2. Molecular structure of $\text{Ba}[\text{C}_5(^i\text{Pr})_5]_2$ [18], the only heavy Group 2 metallocene known that has parallel cyclopentadienyl rings.

Driven in part by newfound applications in materials science [10–13] and organic synthesis [14–17], the number and types of well-characterized organometallic compounds of the heavier Group 2 elements have increased enormously during the last 15 years. During the first part of this period, metallocenes and other cyclopentadienyl-containing compounds dominated the organometallic chemistry of calcium, strontium, and barium. The use of sterically bulky substituents on the rings greatly improved their solubility and ease of manipulation, and most of the structurally verified compounds are of this class. A variety of structural types is now known, such as the monomeric $\text{Ba}[\text{C}_5(^i\text{Pr})_5]_2$ with parallel rings (Fig. 2) [18], the dimeric $[\text{Ca}[\text{C}_5\text{Me}_4\text{Et}](\overline{\text{NSiMe}_2\text{CH}_2\text{CH}_2\text{SiMe}_2})]_2$ (Fig. 3) [19], and the unusual oligomeric $\{\text{Ba}[\text{C}_5(\text{SiMe}_3)_3\text{H}_2]\text{I}(\text{thf})_2\}_x$ (Fig. 4).[20] Organoalkaline-earth metal-

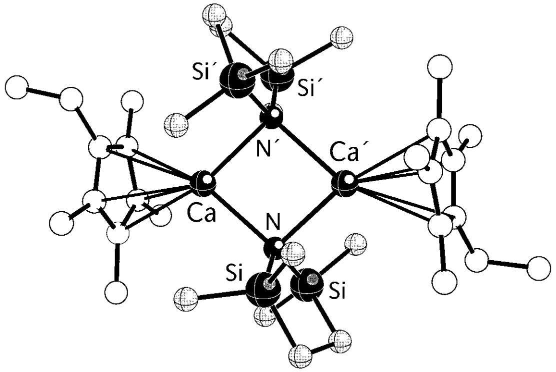

Fig. 3. Structure of the dinuclear $\{\text{Ca}[\text{C}_5\text{Me}_4\text{Et}](\overline{\text{NSiMe}_2\text{CH}_2\text{CH}_2\text{SiMe}_2})\}_2$ [19], whose bridging ligands represent a common structural motif for Cp′AeX molecules.

locenes and related mono(cyclopentadienyl) species AeCp′X (X = halide, amide, alkoxide, etc.) are described in a variety of reviews, including one that covers the early (pre-1980s) literature of the heavy Group 2 metals [21], and several that detail more recent advances in the area [22–27].

The use of bulky ligands has had a similarly invigorating effect on organoalkaline-earth species that do not contain cyclopentadienyl rings. Even though the number of structurally characterized examples is smaller than that of the metallocenes, the distribution of known compounds ranges from those with terminal σ-bonded ligands, to those displaying bridging π-type interactions, to some with Lewis base donor–acceptor contacts. They are helping to dispel the limits that once were thought to circumscribe the chemistry of 'ionic' Group 2 compounds.

### *1.1. Scope of the review*

This article will focus on non-cyclopentadienyl interactions in compounds of calcium, strontium, and barium. By the term 'non-cyclopentadienyl,' we purposely exclude compounds whose only metal-carbon contacts involve the carbocyclic Cp′ ring $[C_5R_nH_{5-n}]^-$ (R = hydrocarbyl, $SiMe_3$, and side chains containing ethers or amines) and various ligands related to it, such as indenyl [28], fluorenyl [29], and silyl- or phosphonium-bridged cyclopentadienes [30,31]. Cyclopentadienyl compounds that support other types of metal–carbon bonds, however, such as $\{Ca[C_5(^iPr)_4H]C{\equiv}CPh(thf)\}_2$ [32], or in which a metal-carbon contact occupies a metal coordination site, such as $\{Ca(C_5Me_5)_2(\mu\text{-}CH_3)_2Al(CH_3)(thf)\}_2$ [33], will be included, although the emphasis will be on the non-Cp′ bonding. For our purposes, five-membered heterocyclic rings, such as phospholes, are not considered cyclopentadienyl ligands, and compounds containing them will be included here.

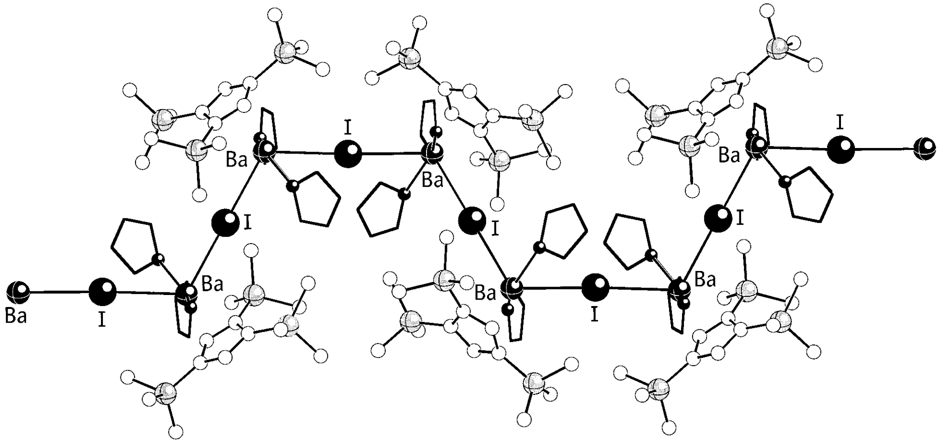

Fig. 4. A chain of the oligomeric $\{Ba[C_5(SiMe_3)_3H_2]I(thf)_2\}_x$ [20], which possesses a zigzag [–Ba–I–Ba′–I′] backbone.

Some classes of compounds covered by this selection (e.g. calcium dialkyls) date from the earliest days of organoalkaline-earth chemistry, but only recently have the structures of several examples been established. Given the long-standing confusion about the constitution of these and other non-cyclopentadienyl complexes, we will focus on those compounds that have been structurally authenticated (which in all cases is by X-ray crystallography). Also covered will be compounds closely related to these, e.g. that differ by the presence or absence of coordinated solvent or in peripheral groups distant from the metal center.

An emphasis on crystallographically characterized species has the unfortunate consequence of highlighting only the most kinetically robust compounds. Such complexes often sport large, metal-shielding ligands, and little reaction chemistry has been described for most of them. There has, however, been increasing synthetic interest in the unusual reactions of organoalkaline-earth species with smaller ligands (e.g. the allylbarium chlorides; see Section 6). Owing to the far more powerful spectroscopic and other characterization tools available to chemists today than to their counterparts of a half-century or more ago, reproducible work with such RAeX compounds is appearing with increasing frequency. Even though the compounds involved have not always been isolated, we believe it is important to describe their reported uses.

For the sake of completeness, we note that radical species containing formal Ca(I) and Sr(I) can be generated from the reactions of calcium and strontium metal vapors with organic oxidizing agents, and include some presumably σ-bonded organometallic species, i.e. $^{\bullet}CaC{\equiv}CH$ and $^{\bullet}CaCH_3$. Density functional theory calculations have been used to compare the structural and spectroscopic attributes of these molecules [34]. This area has been recently reviewed [35], and consequently will not be covered here.

In the next two sections, we include a brief overview of some of the special features of organoalkaline-earth chemistry, and then a synopsis of synthetic methods that have been used to prepare these compounds. Many of these approaches are common to both cyclopentadienyl and non-cyclopentadienyl derivatives; for further details on the former, any of the references [21–27] should be consulted.

## 2. Changes in expectations and models

The location of the heavier alkaline-earth metals in the periodic table might suggest that their compounds share greater similarities with those of magnesium than is actually the case. In fact, however, there is a nearly 40% jump in the radii of the divalent ions on moving from $Mg^{2+}$ (0.72 Å) to $Ca^{2+}$ (1.00 Å), and a further 35% increase on going from $Ca^{2+}$ to $Ba^{2+}$ (1.35 Å) [36]. In addition, the electronegativities of Ca–Ba are quite similar ($\chi = 1.04–0.97$) and notably less than Mg ($\chi = 1.23$) [37]. Such difference combine to make metal–ligand bonds to the heavier metals more polar than to magnesium, and higher coordination numbers are possible with the larger metals. It is consequently not surprising that despite the stoichiometric relationships between the organometallic compounds of magnesium and the calcium subgroup metals (e.g. RMX, $R_2M$), these similarities do not translate into comparable reactivity.

A fruitful model for evaluating the chemistry of calcium, strontium, and barium complexes became available in the late 1970s and early 1980s with the intensive development of organo-f-element chemistry, particularly that of the lanthanide elements [38,39]. Like the heavier alkaline-earth elements, these are also large, highly electropositive metals, and some radii of divalent lanthanide ions are strikingly close to those of the Group 2 elements (i.e. $Ca^{2+} \approx Yb^{2+}$ (1.02 Å), $Sr^{2+} \approx Sm^{2+}$, $Eu^{2+}$ (1.18 Å)). Major advances in f-element chemistry became possible when $[C_5Me_5]^-$, $[CH(SiMe_3)_2]^-$, and other sterically demanding ligands were substituted for $[Cp]^-$ and the smaller alkyl groups (e.g. Me, Et). The larger ligands are more appropriately sized for the f-elements, and confer improved solubility, volatility and thermal stability on their compounds.

As with the lanthanide elements, the use of sterically demanding ligands has greatly increased the accessibility of organoalkaline-earth species. Their properties depend critically on the specific substituents present, however, and blanket characterizations about the properties of certain classes of compounds may not be accurate. For example, the dialkyl complex $Ca[C(SiMe_3)_3]_2$ is synthesized in benzene and is attacked by THF and some ethers ($Et_2O$, PhOEt, $^t$BuOEt),[40] yet the related species $Ca[CH(SiMe_3)_2](thf)_3$ is *prepared* in THF and can be recrystallized from dioxane to yield the stable adduct $Ca[CH(SiMe_3)_2]_2(dioxane)_2$ [41]. Obviously, subtle differences in the steric bulk and donor properties of ligands can strongly affect the reactions of dialkyl compounds, and presumably also of other organoalkaline-earth species. It may be hoped that the accumulation of new structural and reactivity data will eventually clarify the descriptive chemistry of organo-Group 2 compounds.

## 3. Synthetic approaches to Group 2 organometallic compounds

A variety of strategies has been used in the synthesis of alkaline-earth organometallic compounds, beginning with approaches using the elements themselves (e.g. Methods A–C).

$$\mathrm{Ae} + 2\mathrm{RH} \xrightarrow[\text{or NH}_3]{\text{ether, hydrocarbon}} \mathrm{AeR_2} + \mathrm{H_2} \tag{A}$$

$$\mathrm{Ae} + \mathrm{RH} \xrightarrow[\text{hydrocarbon}]{\text{ether or}} \mathrm{AeRH} \tag{B}$$

$$\mathrm{Ae} + \mathrm{RX} \xrightarrow[\text{hydrocarbon}]{\text{ether or}} \mathrm{AeRX}\ (\mathrm{X} = \mathrm{Cl, Br, I}) \tag{C}$$

The metals have been used in the form of vapor [41–43], finely divided powders [14,44] or as 'activated' by amalgamation, treatment with iodine, or ammonia [45]. These approaches represent various attempts to overcome the often low reactivity of the bulk metals, an inertness that apparently stems from facile passivation of the metal surface. For the synthesis of many organoalkaline-earth species, however, the 'activated metal' approach is often not as consistently reliable as others described below.

Synthetic approaches that do not involve the use of elemental forms of the alkaline-earth metals include metathetical (e.g. Methods D, E) and deprotonation reactions (e.g. Method F). These methods generally offer high yields and reproducibility, and removal of the by-products (insoluble alkali metal salts and volatile hexamethyldisilazane, respectively) is usually straightforward. Commonly used starting materials are the anhydrous metal halides or the bis(trimethylsilyl)amides, $Ae[N(SiMe_3)_2]_2(thf)_n$ (Ae = Ca, Sr, Ba; $n$ may be zero) [46,47].

$$M[R] + AeX_2 \xrightarrow[\text{hydrocarbon}]{\text{ether or}} AeRX(ether)_n + MX\downarrow \qquad (D)$$

(M = alkali metal; X = Cl, Br, I (most common); triflate)

$$2M[R] + AeX_2 \xrightarrow[\text{hydrocarbon}]{\text{ether or}} AeR_2(ether)_n + 2\ MX\downarrow \qquad (E)$$

(M = alkali metal; R = Cp′, allyl, COT [48], etc.; X = Cl, Br, I (most common))

$$2RH + Ae[N(SiMe_3)_2]_2(thf)_n \xrightarrow{\text{hydrocarbon}} AeR_2(thf)_n + 2HN(SiMe_3)_2 \qquad (F)$$

Anionic ‘-ate’ complexes are formed from some combinations of reagents (e.g. Methods G–I); lithium-based reagents seem especially prone to these reactions [19,49].

$$(C_5Me_5)_2Ba(thf)_2 + LiL \xrightarrow{\text{toluene}} Li[Ba(C_5Me_5)_2L](thf)_2 \qquad (G)$$

($L = [N(SiMe_3)_2]^-$, $[CH(SiMe_3)_2]^-$)

$$3Li[R] + Ae(SO_2C_6H_4Me\text{-}4)_2 \xrightarrow{\text{THF}} Li[AeR(SO_2C_6H_4Me\text{-}4)_2](thf) \qquad (H)$$

$$3K[R] + Ae(SO_2C_6H_4Me\text{-}4)_2 \xrightarrow{\text{THF}} K[AeR_3](thf)_3 + 2K(SO_2C_6H_4Me\text{-}4)_2\downarrow \qquad (I)$$

The amide ligands of some mono(cyclopentadienyl) complexes can be exchanged to yield new monosubstituted species with metal–carbon σ interactions (e.g. Method J) [32].

$$CaCp'N(SiMe_3)_2(thf) + HC{\equiv}CR \xrightarrow{\text{toluene}} \{CaCp'C{\equiv}CR(thf)\}_n + HN(SiMe_3)_2 \qquad (J)$$

(R = Ph, $SiMe_3$, $Si(^iPr)_3$, ferrocenyl)

In compounds in which Lewis acid–base attractions are the chief metal–ligand binding forces, simple mixing of the reagents in an inert solvent will suffice (e.g. Method K) [50].

$$Ca(C_5Me_5)_2 + nL \xrightarrow{\text{toluene}} Ca(C_5Me_5)_2L_n \qquad (K)$$

($L = RC{\equiv}CR'$; $Me_4\text{–}C_3N_2$; $AlMe_3$)

## 4. Structural studies

One measure of the revival of interest in the organometallic chemistry of the heavier alkaline-earth metals is the increase in published structural determinations during the last two decades. The first example, the solid state structure of $CaCp_2$, was reported in 1974 [9], but not until 1986 was a second described (the gas-phase

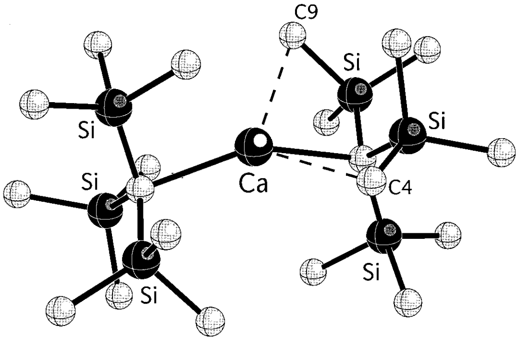

Fig. 5. Structure of the monomeric bent dialkyl complex $Ca[C(SiMe_3)_3]_2$ [40]. The dashed line from the calcium to C9 represents a 3.05 Å contact; that to C4 is 3.12 Å.

geometry of $Ca(C_5Me_5)_2$) [51]. The structure of the first non-cyclopentadienyl complex ($Ca[CH(SiMe_3)_2]_2(dioxane)_2$) was reported only in 1991 [41]. Since then, the number of published structures has constantly grown, and as of this writing, is more than 50. More than a third of these are non-cyclopentadienyl derivatives, which are steadily increasing in variety.

In the descriptions of distinctive structural types that follow, compounds are grouped by ligand type and bonding mode. Anionic hydrocarbyl ligands (both σ- and π-bonded) are first, followed by complexes containing heterocyclic rings. Other complexes displaying metal–carbon contacts are then listed, including metallocarbaboranes and those with various nitrogen containing ligands. At the end are compounds formed between an organoalkaline-earth complex (frequently a metallocene) and a neutral carbon-based donor. Additional details can be found in the references cited in Table 1. In the figures, carbon atoms that are not part of metal-bonded ligands or that are part of cyclopentadienyl rings are represented by open circles.

## *4.1. Sigma-bonded structures*

### *4.1.1. Terminal hydrocarbyls*

*4.1.1.1. $Ca[C(SiMe_3)_3]_2$.* Bis(tris(trimethylsilyl)methyl)calcium is made from the reaction of $K[C(SiMe_3)_3]$ and $CaI_2$ in benzene and crystallizes from heptane–benzene (Method E) [40]. It represents the first (and so far only) crystallographically characterized example of a monomeric base-free dialkyl complex of calcium, and the calcium center possesses the unusually low coordination number of two. As was previously observed with the unsolvated heavy Group 2 metallocenes [52], $Ca[C(SiMe_3)_3]_2$ crystallizes as a bent molecule; its Ca–C distance is 2.459(9) Å and its C–Ca–C angle is 149.7(7)° (Fig. 5). Although this molecule would seem to present an unambiguous example of the non-linear geometries typical of heavy organoalkaline-earth species, the origin of the bending is clouded by several close

Table 1
Structurally characterized non-cyclopentadienyl organocalcium, -strontium and -barium complexes and related species

| Complex | Ae–C distance (av., Å) | Other structural data (distance in Å) | Other characterization | Ref. |
|---|---|---|---|---|
| *Sigma-bonded structures* | | | | |
| Terminally bonded hydrocarbyls | | | | |
| Ca[C(SiMe$_3$)$_3$]$_2$ | 2.459(9) | C–Ca–C′ = 149.7(7)° | NMR ($^1$H, $^{13}$C, $^{29}$Si), mp, MS, el. anal. | [40] |
| Ca[CH(SiMe$_3$)$_2$]$_2$(dioxane)$_2$ | 2.483(5) | Ca–O = 2.373(4);<br>C–Ca–C′ = 133.7(2)°;<br>O–Ca–O′ = 79.4(1)° | NMR ($^1$H, $^{13}$C) | [41] |
| Ca[CH(SiMe$_3$)$_2$]$_2$(thf)$_3$ | | | NMR ($^1$H); converts to bis-dioxane adduct on recryst. from $C_4H_8O_2$ | [41] |
| Ca(C≡CSiPh$_3$)$_2$(18-crown-6) | 2.523(7), 2.558(7) | C–Ca–C′ = 168.7(2)°;<br>Ca–C≡C = 162.4(5), 164.0(5) | NMR ($^1$H); mp, IR | [54] |
| Sr(C≡CSiPh$_3$)$_2$(18-crown-6) | 2.692(4), 2.723(4) | C–Sr–C′ = 166.0(1)°;<br>Sr–C≡C = 158.9(3), 159.7(3) | NMR ($^1$H); mp, IR | [54] |
| Ba(C≡CSiPh$_3$)$_2$(18-crown-6) | 2.852(3), 2.853(2) | C–Ba–C′ = 162.7(1)°;<br>Ba–C≡C = 126.6(3), 141.3(3) | NMR ($^1$H); mp, IR | [54] |
| Bridging hydrocarbyls | | | | |
| {Ca[C$_5$($^i$Pr)$_4$H]C≡CPh(thf)}$_2$ | 2.521(7), 2.551(8) | Ca–C–Ca′ = 93.6(2);<br>C–Ca–C′ = 86.4(2)°; Ca–Cp′ centroid = 2.432 | NMR ($^1$H, $^{13}$C), mp, IR ($\nu_{C\equiv C}$ = 2043 cm$^{-1}$), el. anal. | [32] |
| Ca[C$_5$($^i$Pr)$_4$H]C≡C(C$_5$H$_4$Fe(C$_5$H$_5$))(thf) | | | NMR ($^1$H, $^{13}$C), mp, IR ($\nu_{C\equiv C}$ = 2042 cm$^{-1}$), el. anal. | [32] |
| Ca[C$_5$($^i$Pr)$_4$H]C≡CSiMe$_3$(thf) | | | NMR ($^1$H, $^{13}$C), mp, IR ($\nu_{C\equiv C}$ = 1991 cm$^{-1}$), el. anal. | [32] |
| Ca[C$_5$($^i$Pr)$_4$H]C≡CSiPh$_3$(thf) | | | NMR ($^1$H, $^{13}$C), mp, IR ($\nu_{C\equiv C}$ = 1985 cm$^{-1}$), el. anal. | [32] |
| Ca[C$_5$($^i$Pr)$_4$H]C≡C($^i$Pr)(thf) | | | NMR ($^1$H, $^{13}$C), mp, IR ($\nu_{C\equiv C}$ = 1968 cm$^{-1}$), el. anal. | [32] |

Table 1 (*Continued*)

| Complex | Ae–C distance (av., Å) | Other structural data (distance in Å) | Other characterization | Ref. |
|---|---|---|---|---|
| (Tetrahydrofuran-*O*)barium 2,5-diphenyl-3-(1,4-diphenylbutene-3-yne-2-ide-1-yl)-4-trimethylsilyl-1-phosphacyclopentadienide | On Ba: 3.125(5), ($SiMe_3$–substituted carbon); 3.368(5), 3.033(5) (Me–substituted carbons); 2.899(5); Ba1–C6 3.071(5), Ba1–C6′ 2.881(5), Ba1–C7′ 3.003(6), Ba1–C8′ 3.363(6), Ba1–C41′ = 3.358(5), Ba1–C42′ = 3.356(5) | C–P–C′ = 90.1(3)°; Ba1–C6–Ba1′ = 89.7(1)°; Ba–P = 3.487(2); Ba–O2 = 2.758(4) | NMR ($^1H$, $^{31}P$); mp, IR ($\nu_{C\equiv C} = 1949\ cm^{-1}$), el. anal. | [55] |
| *Pi-bonded structures* | | | | |
| Hydrocarbyl ligands | | | | |
| $Ca[C_5H_3\text{-}1,3\text{-}(SiMe_3)_2]_2(thf)_2$ | 2.654(5) | O1–Ca–O2 = 80.44(13) | NMR ($^1H$, $^{13}C$), mp, IR, el. anal. | [57] |
| Ca(2,3-dimethyl-1,4-diphenyl-1,3-butadiene)$(thf)_4$ | Closest Ca–C(diene) = 2.574(7), 2.588(7) | Inner diene Ca–C = 2.746(7), 2.777(7) Ca–O = 2.40–2.45 | NMR ($^1H$, $^{13}C$); mp, UV–vis | [60] |
| Sr(2,3-dimethyl-1,4-diphenyl-1,3-butadiene)$(thf)_4$ | Closest Sr–C(diene) $^b$ = 2.91(1), 2.87(2); 2.95(2), 2.81(1) | Inner diene Sr–C = 2.91(1), 2.95(2); $^b$ 2.87(2), 2.81(1) Sr–O = 2.55–2.63; 2.60–2.69 $^b$ | NMR ($^1H$, $^{13}C$); mp, UV–vis | [60] |
| $Ca[(^tBu)_2C_5H_5]_2(thf)$ | 2.76(2) | Ca–O = 2.439(9) | NMR ($^1H$); el. anal. | [61] |
| $Ba[Ph_2P(4\text{-}MeC_6H_5CH)]_2$ | Ba–C(ylidic) = 3.217(7), 3.106(7), 3.299(8), 3.454(6); $Ba–C_{ipso}$ = 2.981(6), 3.031(6), 3.014(6), 3.003(6); $Ba–C_{ortho}$ = 3.159(6), 3.193(7), 3.155(7), 3.074(7) | Ba–P(1) = 3.714(6), Ba–P(2) = 3.944(6); C–P(1)–C′ = 115.9(3)°, C–P(2)–C′ = 116.7(4)° | NMR ($^1H$, $^{13}C$) | [67] |
| Ba{$\eta^5$-PhCH($C_5H_4N$-2)}$_2$ (diglyme)(thf) | Ba–C/N = 2.983(6), 3.156(6) Å; $Ba–C_{ipso}$ = 3.146(7), 3.138(7); $Ba–C_{intermediate}$ = 3.245(6), 3.223(7); 3.215(6), 3.303(6) | Ba–O(thf) = 2.819(4); Ba–O(diglyme) = 2.800(4), 2.855(4), 2.766(4) | NMR ($^1H$), mp, el. anal. | [68] |

Table 1 (*Continued*)

| Complex | Ae–C distance (av., Å) | Other structural data (distance in Å) | Other characterization | Ref. |
|---|---|---|---|---|
| *Heterocyclic compounds* | | | | |
| $\{(\eta^5\text{-PC}_4(2,5\text{-SiMe}_3)_2(3,4\text{-Me})_2)\text{Ca(thf)}_2(\mu\text{-C}_5\text{H}_5)\text{Ca}(\eta^5\text{-PC}_4(2,5\text{-SiMe}_3)_2(3,4\text{-Me})_2)(\mu\text{-Cl})\}_2$ | On Ca1: 2.826(5), 2.813(6) ($\text{SiMe}_3$–substituted carbon); 2.793(5), 2.733(5); to μ-Cp (2.76). On Ca2: 2.832(5), 2.816(5) ($\text{SiMe}_3$–substituted carbon); 2.871(5), 2.862(5); to μ-Cp (2.79) | C–P–C′ = 91.8(2)°;<br>Ca–Cl = 2.826(5), 2.813(6);<br>Ca2–Cl–Ca2′ = 95.13(5)°,<br>Ca–O4 = 2.406(4),<br>Ca–O5 = 2.362(4) | NMR ($^1$H, $^{29}$Si, $^{31}$P); mp (dec.), IR | [69] |
| $\{(\eta^5\text{-AsC}_4(2,5\text{-SiMe}_3)_2(3,4\text{-Me})_2)\text{-Ca}(\mu\text{-Cl})(\text{thf})_2\}_2$ | 2.832(3), 2.903(4) ($\text{SiMe}_3$–substituted carbon); 2.770(3), 2.817(3) | C–As–C′ = 87.9(2)°;<br>Ca–Cl = 2.714(1), 2.724(1);<br>Cl–Ca–Cl′ = 79.25(3)°,<br>Ca–O1 = 2.408(3),<br>Ca–O2 = 2.411(2) | NMR (1H, 29Si); mp (dec.), IR, el. anal. | ADDIN ENRfu [69] |
| $\text{Ba}_2\{(\text{C}_6\text{H}_{11})\text{NC(Me)CHC(Me)N}\text{–}(\text{C}_6\text{H}_{11})\}_3\{(\text{SiMe}_3)_2\text{N}\}$ | Ba2–C(50, 49, 47) = 3.16, 3.20, 3.24; Ba–C(13, 15) = 3.19, 3.12; Ba2–C(30, 32, 33) = 3.41, 3.34, 3.21 | Ba1–N4 = 2.829(4);<br>Ba1–N5 = 2.841(4);<br>Ba2–N4 = 2.860(4);<br>Ba2–N5 = 3.108(4),<br>Ba2–N7 = 635(4);<br>Ba1–N2 = 2.613(4) | NMR ($^1$H), mp, el. anal. | [71] |
| *Other complexes* | | | | |
| Metallocarbaboranes | | | | |
| *closo*-$(\text{MeCN})_4\text{-1,2,4-CaC}_2\text{B}_{10}\text{H}_{12}$ | 2.701(5), 2.895(5) | Ca–B = 2.65–2.94<br>Ca–N = 2.43–2.51 | NMR ($^1$H, $^{11}$B); mp, IR, el. anal. | [72] |
| $\{$*closo*-$(\text{MeCN})_3\text{-1,2,4-SrC}_2\text{B}_{10}\text{H}_{12}\}_n$ | 2.997(10) (3.064(10)) [b]; 3.176(10) (3.142(11)) [b] | Sr···H–C = 2.62(9) (2.70(8)) [b];<br>Sr···H–B = 2.56(9) (2.87(9)) [b]<br>Sr–B = 2.87–3.13; 2.83–3.06 [b];<br>Sr–N = 2.63–2.77; 2.69–2.70 [b] | NMR ($^1$H, $^{11}$B); IR | [73] |

Table 1 (*Continued*)

| Complex | Ae–C distance (av., Å) | Other structural data (distance in Å) | Other characterization | Ref. |
|---|---|---|---|---|
| $\{closo\text{-(thf)}_3\text{-1,2,4-SrC}_2\text{B}_{10}\text{H}_{12}\}_n$ | | | IR; converts to *tris*-MeCN adduct on recryst. from $MeCN/Et_2O$ | [73] |
| *Lewis acid–base adducts* | | | | |
| $Ca(C_5Me_5)_2(Me_3SiC{\equiv}C{-}C{\equiv}CSiMe_3)$ | 2.991(5), 3.024(5), (in ‘Å’) [c]<br>2.878(5), 3.104(5), (in ‘B’) [c] | Ca–C (Cp′) = 2.65(3) [a] | NMR ($^1H$, $^{13}C$); IR | [50] |
| $Ca(C_5Me_5)_2(MeC{\equiv}C{-}C{\equiv}CMe)$ | 2.87(2), 2.92(2), (in ‘Å’) [c]<br>2.92(2), 2.95(2), (in ‘B’) [c] | Ca–C (Cp′) = 2.65(5) [a] | NMR ($^1H$) | [74] |
| $Ca(C_5Me_5)_2(1,3,4,5\text{-}Me_4{-}C_3N_2)$ | 2.562(2) | Ca–Cp′ centroid = 2.384, 2.381 | NMR ($^1H$, $^{13}C$), mp, el. anal. | [75] |
| $Sr(C_5Me_5)_2(1,3,4,5\text{-}Me_4{-}C_3N_2)$ | | | NMR ($^1H$, $^{13}C$), mp, el. anal. | [75] |
| $Ba(C_5Me_5)_2(1,3,4,5\text{-}Me_4{-}C_3N_2)$ | 2.951(3) | Ca–Cp′ centroid = 2.741, 2.735 | NMR ($^1H$, $^{13}C$), mp | [75] |
| $Sr(C_5Me_5)_2(1,3,4,5\text{-}Me_4{-}C_3N_2)_2$ | 2.868(5), 2.854(5) | Ca–Cp′ centroid = 2.655, 2.669<br>C–Sr–C′ = 86.4(1)° | NMR ($^1H$, $^{13}C$), mp | [75] |
| $Ba(C_5Me_5)_2(1,3,4,5\text{-}Me_4{-}C_3N_2)_2$ | | | NMR ($^1H$, $^{13}C$), mp | [75] |
| $[(C_5Me_5)_2Ca(\mu\text{-}CH_3)_2Al(CH_3)(thf)]_2$ | $(Ca{\cdots}C(H_3)$ = 2.948(7), 2.999(7) | Ca–C (Cp′) = 2.70(1) | NMR ($^1H$), IR, el. anal. | [33] |
| $Ba[(3,5\text{-dimethylpyrazol-1-yl})_3Ge]_2(dioxane)_{1/2}$ | av Ba–C12/C27 = 3.393; av Ba–C14/C29 = 3.275 | av Ba–N(σ) = 2.80(3)<br>Ba–N5/N11 = 2.967;<br>Ba–N6/N12 = 2.927 | NMR ($^1H$), IR, mp, MS, el. anal. | [78] |

[a] Two independent molecules exist in the unit cell; the average value is given.

[b] Two independent molecules exist in the unit cell; the values are not averaged.

[c] The two closest Ca–C(methyne) contacts.

intramolecular contacts, in particular, Ca···C(Me) distances of ca. 3.0 Å. These generate Ca···H distances of roughly 2.5 Å. The importance of these contacts is difficult to gauge, although the Ca···C(Me) separations are not far from the Ca–μ($CH_3$) distances observed in {$Ca(C_5Me_5)_2(\mu\text{-}CH_3)_2Al(CH_3)(thf)\}_2$ (2.948(7), 2.999(7) Å) [33], and the Ca···H contacts are similar to the Ca···H(α-$CH_2$) separation observed in $Ca[1,2,4\text{-}C_5(SiMe_3)_3H_2](HBEt_3)(thf)_2$ (2.41 Å), which is energetically significant [53]. The synthesis and structural characterization of more solvent-free $AeR_2$ complexes are needed to clarify this feature of Group 2–carbon bonding.

*4.1.1.2. $Ca[CH(SiMe_3)_2]_2(dioxane)_2$.* Bis(bis(trimethylsilyl)methyl)calcium has been isolated from the metal-vapor reaction of calcium with $BrCH(SiMe_3)_2$ in THF at 77 K (Method C) [41]. It is possible that a Grignard-like species (i.e. $Ca[CH(SiMe_3)_2]Br(thf)_n$) is initially formed that through Schlenk rearrangement yields $Ca[CH(SiMe_3)_2]_2(thf)_3$ and $CaBr_2(thf)_n$. Recrystallization of the former from 1,4-dioxane gives crystals of the disolvate. The compound exists as a monomer with a crystallographically imposed $C_2$ axis through the metal center (Fig. 6). The tetrahedral metal environment is distorted, with Ca–C = 2.483(5) Å, Ca–O = 2.373(4) Å, C–Ca–C′ angle = 133.7(2)° and O–Ca–O′ = 79.4(1)°.

*4.1.1.3. $Ae(C{\equiv}CSiPh_3)_2(18\text{-}crown\text{-}6)$ (Ae = Ca, Sr, Ba).* The reaction of the bulky amido complexes $Ae[N(SiMe_3)_2]_2$ [54] with triphenylsilylethyne in the presence of the cyclic ether 18-crown-6 leads to the formation of the bis(acetylide) compounds for all three calcium subgroup metals (Method F) (Fig. 7). The compounds are monomers, with terminal acetylides (Ca–C = 2.523(7), 2.558(7) Å; Sr–C = 2.692(4), 2.723(4) Å; Ba–C = 2.852(3), 2.853(2) Å); the anionic ligands can be viewed (structurally, not mechanistically) as having been threaded through the crown ether. All three compounds display bent C–Ae–C′ and Ae–C≡C angles. The C–Ae–C′ angles slightly decrease with increasing size of the metal (168.7(2)° (Ca); 166.0(1)°

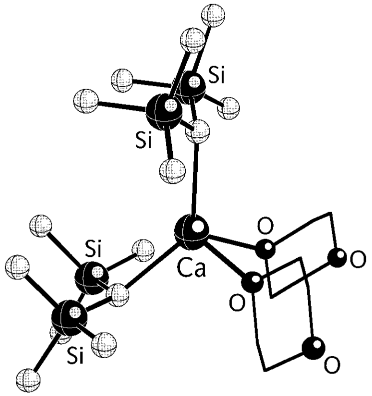

Fig. 6. Structure of the monomeric dialkyl complex $Ca[CH(SiMe_3)_2]_2$ (dioxane)$_2$ [41].

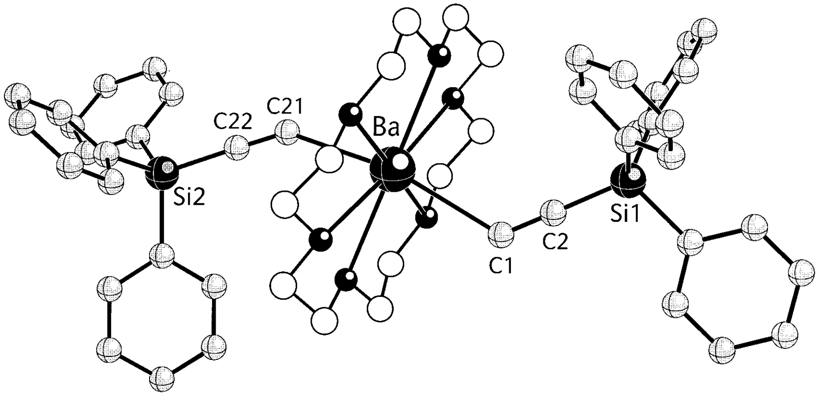

Fig. 7. Structure of the bis(acetylide) complex $Ba(C{\equiv}CSiPh_3)_2$(18-crown-6) [54].

(Sr); 162.7(1)° Ba). The Ae–C≡C angles change more dramatically, from near 160° for Ae = Ca and Sr, to 126.6(3) and 141.3(3)° in the barium compound. The bending is such in the barium compound that the possibility of some side-on Ba($\eta^2$-C≡CR) bonding has to be considered; as it has the largest metal coordination environment, the barium complex can accommodate such a configuration most easily.

### 4.1.2. Bridging hydrocarbyls

*4.1.2.1. {Ca[$C_5(^iPr)_4H$]C≡CPh(thf)}$_2$.* This compound is one of a family of compounds formed by protonolysis of $Ca[C_5(^iPr)_4H]N(SiMe_3)_2$(thf) with RC≡CH (R = Ph, ferrocenyl, $SiMe_3$, $Si(^iPr)_3$, and $SiPh_3$) (Method J), and it provides an example of the solution stability conferred on mono(cyclopentadienyl) complexes by the 'encapsulating' $[C_5(^iPr)_4H]^-$ ring [32]. The R = phenyl derivative complex exists as a centrosymmetric dimer, with a bridging –C≡CPh ligand and a coordinated thf completing each metal coordination environment (Fig. 8). The Ca–C–Ca′–C core is almost square, with Ca–μ-C distances of 2.521(7) and 2.551(8) Å, and Ca–C–Ca′ and C–Ca–C′ angles of 93.6(2) and 86.4(2)°, respectively.

*4.1.2.2. (Tetrahydrofuran-O)barium 2,5-diphenyl-3-(1,4-diphenylbutene-3-yne-2-ide-1-yl)-4-trimethylsilyl-1-phosphacyclopentadienide.* This unusual compound defies simple categorization as to method of formation or structure type, as it contains Ba–C σ bonds, side-on Ba–alkyne and arene interactions, and Ba–phospholide bonds [55]. The reaction of $Ba[P(SiMe_3)_2]_2(thf)_2$ with diphenylbutadiyne in toluene for 12 days induces a *cis*-addition of the diyne to the phosphide, followed by a 1,3-silyl group shift and ring closure, and leads to the isolation of (tetrahydrofuran-*O*)barium 2,5-diphenyl-3-(1,4-diphenylbutene-3-yne-2-ide-1-yl)-4-trimethylsilyl-1-phosphacyclopentadienide in good yield. The compound crystallizes as a dimer around a nearly square $Ba_2C_2$ core with Ba–C and Ba–C′ distances of 2.881(5) and

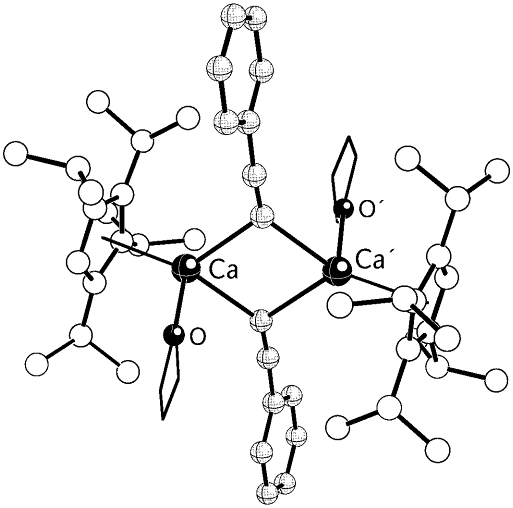

Fig. 8. Structure of the dimeric phenylacetylide complex $\{Ca[C_5(^iPr)_4H]C{\equiv}CPh(thf)\}_2$ [32].

2.899(5) Å, respectively, and Ba–C6–Ba′ = 89.7(1)° (Fig. 9). The Ba–phospholide coordination is highly asymmetric, with distances ranging from Ba–P at 3.487(2) Å to Ba–C lengths from 2.899(5) (Ba–C3) to 3.368(5) Å (Ba–C1). There are long contacts to two of the carbons of a phenyl group on the phosphole at 3.358(5) and 3.356(5) Å. The C7–C8 alkyne fragment off the phospholide binds in a side-on fashion to the barium, with Ba–C7 and Ba–C8 distances of 3.003(6) and 3.363(6) Å,

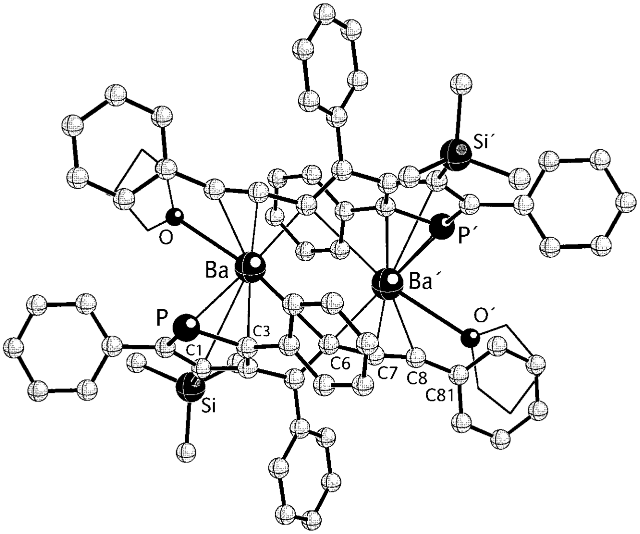

Fig. 9. Structure of the bimetallic complex (tetrahydrofuran-*O*)barium 2,5-diphenyl-3-(1,4-diphenylbutene-3-yne-2-ide-1-yl)-4-trimethylsilyl-1-phosphacyclopentadienide [55].

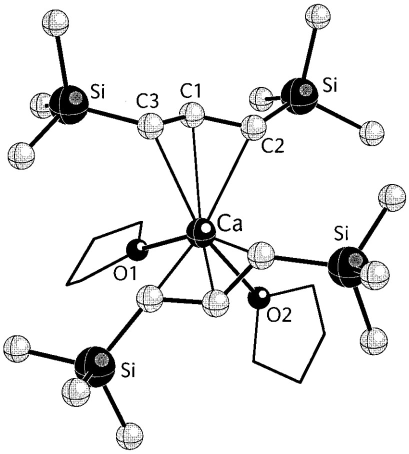

Fig. 10. Structure of the monomeric bis(allyl) complex $Ca[C_3(SiMe_3)_2H_3]_2 \cdot (thf)_2$ [57].

respectively; accompanying this coordination is a $\nu_{C \equiv C}$ of 1949 $cm^{-1}$ (reduced from 2150 $cm^{-1}$ [56]) and distinctly bent C6–C7–C8 and C7–C8–C81 angles of 167.6(6) and 160.4(6)°, respectively.

### 4.2. Pi-bonded structures

### 4.2.1. Hydrocarbyl ligands

*4.2.1.1. $Ca[C_3(SiMe_3)_2H_3]_2(thf)_2$.* The allyl anion represents the simplest π-delocalized ligand, and although some allylbarium compounds have been described (see Section 6), the allyl–(Ca,Sr,Ba) bond has been crystallographically characterized in only one bis(allyl) complex of calcium. Reaction of slightly more than two equivalents of $K[C_3(SiMe_3)_2H_3]$ with $CaI_2$ in THF produces the colorless complex $Ca[C_3(SiMe_3)_2H_3]_2(thf)_2$ in high yield (Method E) [57]. The $^1H$-NMR spectrum of the complex is invariant from room temperature (r.t.) to 172(2) K, suggesting that the molecule is either nonfluxional or the rearrangements are of low energy. The complex crystallizes with a crystallographically imposed $C_2$ axis through the calcium atom (Fig. 10); the two allyl ligands are in an *anti*-configuration, and the angle between the $C_3$ planes is 115.5°. The C–C bonds in the allyl ligand are essentially the same length at 1.402(4) Å (C1–C2) and 1.387(4) Å (C1–C3).

The allyl ligands are bound in a symmetrical *trihapto* manner to the metal, with an average Ca–C distance of 2.654(5) Å and a spread of only 0.014 Å. The hydrogen atoms clearly lie out of the plane of the allyl carbon atoms: the C3–C1–C2–H2 torsion angle is 16.9°, that for C2–C1–C3–H3 is 16.2°, and the central C1–H1 bond is tipped toward the calcium atom, and forms an angle of 12.8° with the $C_3$ plane. Such hydrogen atom displacements are similar to those calculated or found in other main-group and transition metal allyl structures such as $Cs(C_3H_5)$ [58] or bis($\eta^3$-allyl)nickel [59]. This atomic arrangement has been attributed to the relief of steric interaction between the metal and the allylic hydrogens and to rehybridization of the allyl carbon atoms to improve metal–ligand bonding.

*4.2.1.2. Ae(2,3-Dimethyl-1,4-diphenyl-1,3-butadiene)(thf)$_4$ (Ae = Ca, Sr).* The transition from oligomeric to monomeric complexes can sometimes hinge on small increases in the steric bulk of ligands. For example, although the calcium derivative of 1,4-diphenyl-1,3-butadiene is believed to be oligomeric, the addition of two methyl groups causes the deep red 2,3-dimethyl-1,4-diphenyl-1,3-butadiene complex, formed from the reaction of the metal with the hydrocarbon in THF (Method A), to be monomeric [60]. The structures of the calcium- and strontium-butadienyl complexes are intermediate between those of ‘face on’ $\eta^4$-dienes and ‘side on’ ($\eta^2$-coordinated) metallacyclo-3-pentenes. In the calcium complex (Fig. 11), the Ca is coordinated in a distorted octahedral environment by four thf molecules and the butadiene moiety. The Ca–C bond distances involving the outer carbons of the diene (Ca–C1 = 2.574(7), Ca–C4 = 2.588(7) Å) are substantially shorter than those to the inner carbons (Ca–C2 = 2.746(7); Ca–C3 = 2.777(7) Å), and there is considerable localization of the bonding (e.g. C1–C2 and C3–C4 = 1.448(9) and 1.472(9) Å, respectively, but C2–C3 = 1.375(8) Å). In the solid state, the diene is coordinated in an (*E*,*Z*) fashion, but in solution an equilibrium is observed between the (*E*,*Z*) form and a more symmetrical (*E*,*E*) arrangement, which is preferred at low temperature (−60°C).

In both of the two crystallographically independent but closely similar strontium complexes (Fig. 12), the Sr is also coordinated in a distorted octahedral environment by four thf molecules and the butadiene moiety. The M–C bond distances involving the outer carbons of the diene (Sr–C1 = 2.73(2), Sr–C4 = 2.71(1) Å) are appreciably shorter than those to the inner carbons (Sr–C2 = 2.91(1); Sr–C3 = 2.95(2) Å), and there is localization of the bonding in the diene fragment (C1–C2

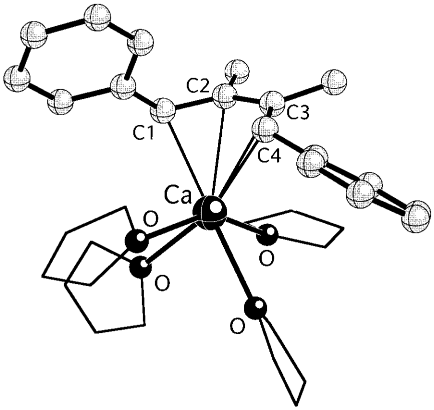

Fig. 11. Structure of the monomeric butadienyl complex Ca(2,3-dimethyl-1,4-diphenyl-1,3-butadiene)(thf)$_4$ [60].

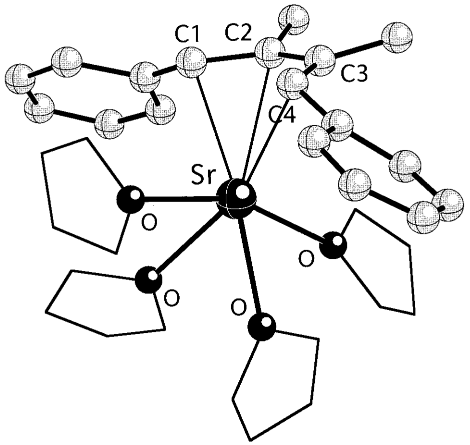

Fig. 12. Structure of the monomeric bis(allyl) complex Sr(2,3-dimethyl-1,4-diphenyl-1,3-butadiene) $(thf)_4$ [60].

and C3–C4 = 1.48(2) and 1.47 (2) Å, respectively, and C2–C3 = 1.38(2) Å). Unlike the arrangement observed in the calcium complex, however, the two phenyl rings bend toward the metal, leading to Sr···C(phenyl) contacts as close as 3.16 Å. These may represent weak σ-type interactions.

*4.2.1.3.* *$Ca[C_5(^tBu)_2H_5]_2(thf)$*. The only structurally characterized example of a pentadienyl complex of the heavier alkaline-earth metals, $Ca[C_5(^tBu)_2H_5]_2(thf)$ is prepared from $K[C_5(^tBu)_2H_5]$ and $CaI_2$ in THF (Method E). It crystallizes with two planar $\eta^5$-pentadienyl ligands (Ca–C distances range from 2.74(1) to 2.81(2) Å) and a coordinated thf molecule (Fig. 13) [61]. The pentahapto coordination of the

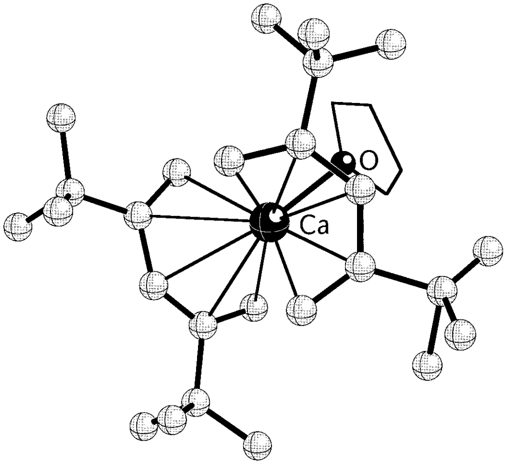

Fig. 13. Structure of the monomeric ‘open calcocene’ $Ca[(^tBu)_2C_5H_5]_2(thf)$ [61].

dienyl ligands distinguishes this 'open calcocene' from other structurally characterized main-group pentadienyl complexes, which have σ-bonded, monohapto ligands [62]. Interestingly, the average Ca–C bond distance is longer than the values in seven-coordinate cyclopentadienyl complexes [63–65]. Transition metal pentadienyl complexes, in contrast, typically have M–C distances that are equal to, or shorter than, distances in metal-cyclopentadienyl complexes [66].

The nearly '*anti*-eclipsed' configuration of the pentadienyl ligands (174.4° twist angle) has not previously been observed in an open metallocene; values in transition metal complexes usually range from 60° ('*gauche*-eclipsed') to 90° [66]. Steric strain from the $^t$Bu groups probably does not force the *anti*-eclipsed arrangement, as the closest contact between them is 4.28 Å, which is well outside the sum of van der Waals radii.

#### *4.2.1.4. Ba[Ph$_2$P(4-MeC$_6$H$_5$CH)]$_2$.*

The phosphonium bromide [Ph$_2$P(4-MeC$_6$H$_5$CH$_2$)$_2$]Br is deprotonated with KN(SiMe$_3$)$_2$ in THF to form the corresponding nuetral ylide, Ph$_2$P(4-MeC$_6$H$_5$CH)(4-MeC$_6$H$_5$CH$_2$). The latter reacts with the amido complex Ba[N(SiMe$_3$)$_2$]$_2$ in THF at 60°C to yield the orange Ba[Ph$_2$P(4-MeC$_6$H$_5$CH)]$_2$ (Method F) [67]. The formally 12-coordinate barium center is coordinated by four benzyl ligands, each in an η$^3$-fashion (Fig. 14); the two ligands have $C_2$ symmetry but opposite chirality, so that the whole complex has approximate $S_4$ symmetry. The actual Ba–C contacts span a large range, and are not all grouped in easily recognized sets. The carbon atoms adjacent to the ylidic carbons (C12, C22, C52, C62) do have the shortest contacts (2.981(6)–3.031(6) Å), but the barium–ylidic carbon distances range from 3.106(7) Å (Ba–C21) to 3.454(6) Å

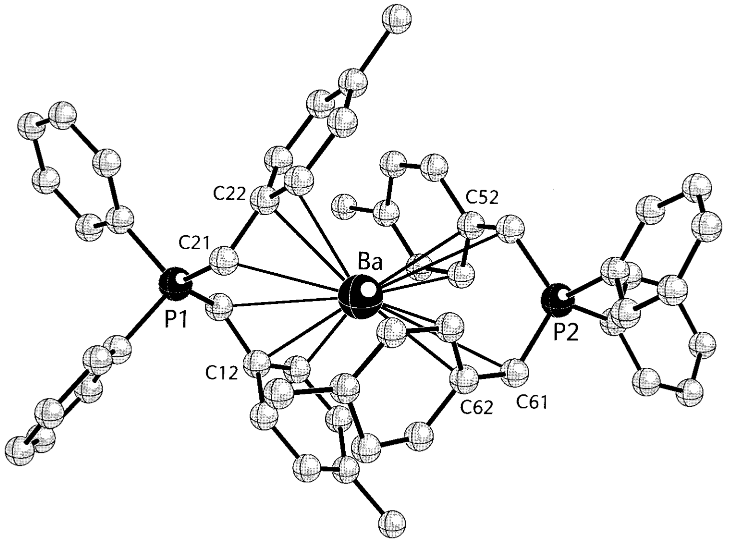

Fig. 14. Structure of the phosphonium dibenzylide complex Ba[Ph$_2$P(4-MeC$_6$H$_5$CH)]$_2$ [67].

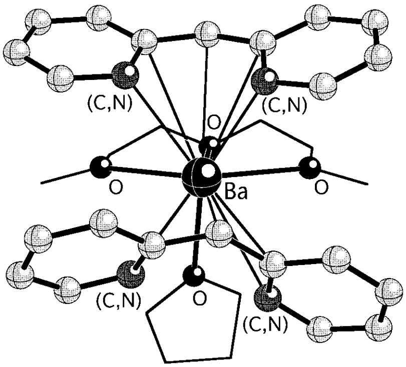

Fig. 15. Structure of the pyridylphenylmethane complex Ba{$\eta^5$-PhCH($C_5H_4N$-2)}$_2$(diglyme)(thf) [68].

(Ba–C61); the latter is on the edge of what could be considered a significant interaction. The molecule is fluxional in solution, and the rearrangement involves rotation of the benzylide rings and possible disruption of the Ba–ylide interaction, transiently lowering the symmetry to $D_2$. Ab initio calculations are consistent with a high degree of ionicity in the complexes; in particular, the distortion in the benzylide rings (contraction of the bond angles at the *ipso* and *para* carbons, and a widening at the *ortho* and *meta* carbons), are similar to those predicted for the free $[H_2P(CHPh)_2]^-$ anion.

*4.2.1.5. Ba[$\eta^5$-PhCH($C_5H_4N$-2)]$_2$(diglyme)(thf).* Metallation of 2-pyridylphenylmethane and barium in liquid ammonia in the presence of diglyme and thf (Method A) affords the red Ba[$\eta^5$-PhCH($C_5H_4N$-2)]$_2$(diglyme)(thf) [68]. The barium is coordinated by two 2-pyridylphenylmethyl groups in an $\eta^5$-manner, the trihapto diglyme ligand, and a thf molecule (Fig. 15). The pentahapto binding of the anionic groups prompted the description of the compound as a bent 'open barocene,' although the term *open metallocene* is usually restricted to compounds containing coordinated pentadienyl ligands [66]. Disorder in the 2-pyridylphenylmethyl ligands, which are bound in an *anti*-eclipsed fashion, make it impossible to distinguish between the nitrogen atoms and the intraligand phenyl C–H centers. Within each anionic ligand, the Ba–C/N distances are the shortest (2.983(6), 3.156(6) Å), followed by the central *ipso* carbons (3.146(7), 3.138(7) Å), and then the intermediate carbons (3.245(6), 3.223(7); 3.215(6), 3.303(6) Å). The pyridyl and phenyl rings are roughly parallel to each other in the anionic ligands (dihedral angles of 16.0 and 21.8°), and the central *ipso* carbon is involved in delocalized bonding ($C_{ipso}$–C distances range from 1.41(1) to 1.43(9) Å), but the rings themselves are tipped away from the barium atom.

### 4.2.2. Heterocyclic compounds

*4.2.2.1. $\{(\eta^5\text{-}PC_4(2,5\text{-}SiMe_3)_2(3,4\text{-}Me)_2)Ca(thf)_2(\mu\text{-}C_5H_5)Ca(\eta^5\text{-}PC_4(2,5\text{-}SiMe_3)_2\text{-}(3,4\text{-}Me)_2)(\mu\text{-}Cl)\}_2$.* The reaction of 1,1-bis(cyclopentadienyl)-3,4-dimethyl-2,5-bis(trimethylsilyl)-1-zirconacyclopenta-2,4-diene with $PCl_3$ yields an inseparable mixture of 1-chloro- and 1-cyclopentadienyl-3,4-dimethyl-2,5-bis(trimethylsilyl)-1-phosphacyclopenta-2,4-diene. Subsequent reaction of the mixture with distilled calcium metal for 6 days produces the tetranuclear $\{(\eta^5\text{-}PC_4(2,5\text{-}SiMe_3)_2(3,4\text{-}Me)_2)Ca(thf)_2(\mu\text{-}C_5H_5)Ca(\eta^5\text{-}PC_4(2,5\text{-}SiMe_3)_2(3,4\text{-}Me)_2)(\mu\text{-}Cl)\}_2$ (Method C) (Fig. 16) [69]. The centrosymmetric $Ca_2Cl_2$ core is nearly square, with Ca–Cl distances of 2.826(5) and 2.813(6) Å, and an Ca2–Cl–Ca2′ angle of 95.13(5)°. The phospholide anion is planar and delocalized, with average P–C bonds of 1.78 Å, nearly equal C–C bonds (av 1.42 Å), and a C–P–C′ angle of 91.8(2)°. The Ca–phospholide distances range from Ca1–P at 2.933(2) Å and Ca2–P at 2.912(2) Å, to an average of 2.805 Å for Ca1–C and 2.845 Å for Ca2–C. Distances to the bridging $C_5H_5$ ring (av 2.76 Å for Ca1–Cp; av 2.79 Å for Ca2–Cp) are close to the range expected for eight-coordinate calcium [70].

*4.2.2.2. $\{(\eta^5\text{-}AsC_4(2,5\text{-}SiMe_3)_2(3,4\text{-}Me)_2)Ca(\mu\text{-}Cl)(thf)_2\}_2$.* In an unusual series of reactions, 1,1-bis(cyclopentadienyl)-3,4-dimethyl-2,5-bis(trimethylsilyl)-1-zirconacyclopenta-2,4-diene reacts with $AsCl_3$ to yield 1-chloro-3,4-dimethyl-2,5-bis(trimethylsilyl)arsole. Reduction of the latter with distilled calcium metal produces the dimeric $\{(\eta^5\text{-}AsC_4(2,5\text{-}SiMe_3)_2(3,4\text{-}Me)_2)Ca(\mu\text{-}Cl)(thf)_2\}_2$ (Method C) (Fig. 17) [69]. The centrosymmetric $Ca_2Cl_2$ core has nearly equal Ca–Cl distances of

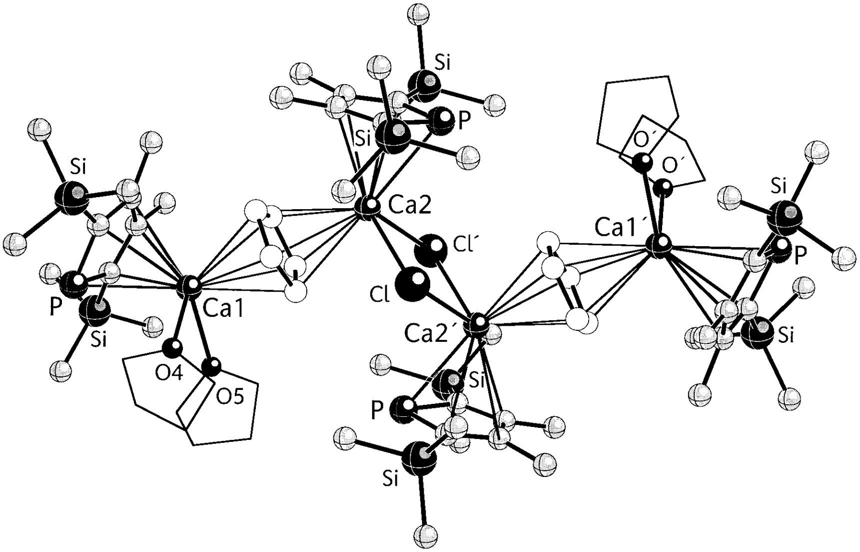

Fig. 16. Structure of the tetranuclear complex $\{[(\eta^5\text{-}PC_4(2,5\text{-}SiMe_3)_2(3,4\text{-}Me)_2)Ca(thf)_2(\mu\text{-}C_5H_5)Ca(\eta^5\text{-}PC_4(2,5\text{-}SiMe_3)_2(3,4\text{-}Me)_2)(\mu\text{-}Cl)\}_2$ [69].

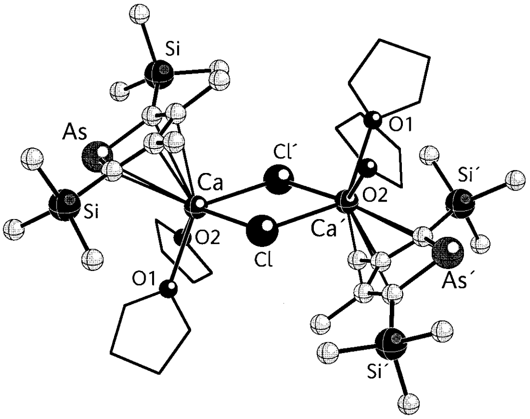

Fig. 17. Structure of the dimeric complex $\{[(\eta^5\text{-AsC}_4(2,5\text{-SiMe}_3)_2(3,4\text{-Me})_2)\text{Ca}(\mu\text{-Cl})(\text{thf})_2\}_2$ [69].

2.714(1) and 2.724(1) Å, and an Cl–Ca–Cl′ angle of 79.25(3)°. The arsolide anion is planar, with nearly equal C–C bonds (av 1.41 Å), As–C distances of 1.892(5) Å, and a C–As–C′ angle of 87.9(2)°. The Ca–arsolide distances are, as expected, unequal, ranging from Ca–As of 3.0737(8) Å, to 2.832(3) and 2.903(4) Å for the trimethylsilyl-substituted carbons, to 2.770(3) and 2.817(3) Å for the methyl-substituted carbons.

### 4.2.3. Other compounds

*4.2.3.1.* $Ba_2[(C_6H_{11})NC(Me)CHC(Me)N(C_6H_{11})]_3\{(SiMe_3)_2N\}$. The reaction of $Ba\{N(SiMe_3)_2\}_2(thf)_2$ with $(C_6H_{11})NHCMeCHCMeN(C_6H_{11})$ in petroleum ether yields the diazapentadienyl (DAP) compound $Ba_2[(C_6H_{11})NC(Me)\text{-}CHC(Me)N(C_6H_{11})]_3\{(SiMe_3)_2N\}$ (Method F) [71]. The dimeric complex retains a bis(trimethylsilyl)amido group from the starting barium amide, and contains three DAP ligands that display different coordination modes (Fig. 18). One of these is bonded in a terminal mode to Ba2, with Ba–C bonds of ca. 3.2 Å, although the primary interaction is with N6 and N7 at 2.689(4) and 2.635(4) Å, respectively. A second DAP ligand spans Ba1 and Ba2 and adopts a ‘W’ conformation. The principal bonding is again through the nitrogen atoms (Ba1–N2 = 2.613(4), Ba2–N3 = 2.873(4) Å), although there are long range Ba–C contacts of 3.1–3.2 Å (to C13, C15). Finally, a third DAP ligand is turned perpendicularly to the Ba1–Ba2 vector, and adopts a π-bonded orientation to Ba2, though the Ba2–C(30, 32, 33) bonds are long at 3.41, 3.34, and 3.21 Å, respectively. The plane of the DAP ligand is tipped toward Ba2, apparently to relieve steric crowding with the cyclohexyl groups of the other bridging DAP ligand.

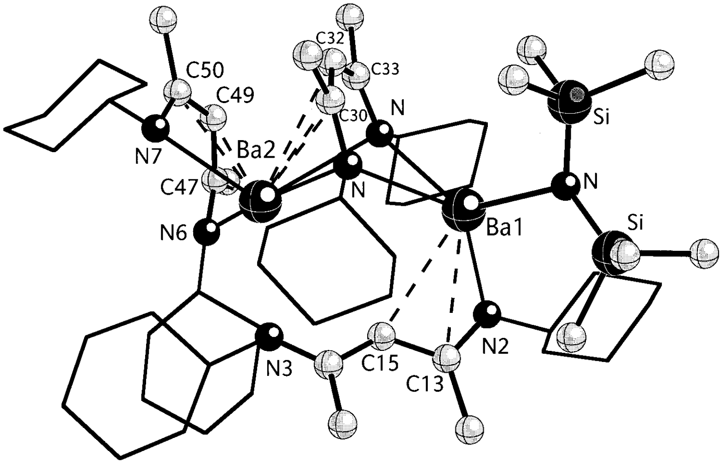

Fig. 18. Structure of the dimeric complex $Ba_2[(C_6H_{11})NC(Me)CHC(Me)N(C_6H_{11})\}_3[(SiMe_3)_2N]$ [71].

## 4.3. *Other complexes*

### 4.3.1. *Metallocarbaboranes*

*4.3.1.1. closo-$(MeCN)_4$-1,2,4-$CaC_2B_{10}H_{12}$.* The reaction of $Na_2$[*nido*-7,9-$C_2B_{10}H_{12}$] with $CaI_2$ in THF at r.t. precipitates a colorless solid that on recrystallization from $MeCN-Et_2O$ yields the monomeric *closo*-$(MeCN)_4$-1,2,4-$CaC_2B_{10}H_{12}$ (Method D) (Fig. 19) [72]. The calcium atom caps the open face of the carbaborane, and is coordinated by four acetonitrile ligands. The Ca–C distances are distinctly unequal at 2.70 and 2.89 Å, and the Ca–B lengths range from 2.65 to 2.94 Å; this produces a puckered six-membered ring. The Ca–N contacts vary from 2.43 to 2.51 Å.

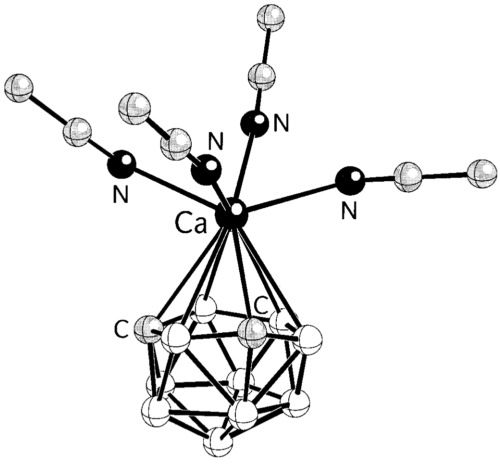

Fig. 19. Structure of the monomeric metallacarbaborane *closo*-$(MeCN)_4$-1,2,4-$CaC_2B_{10}H_{12}$ [72].

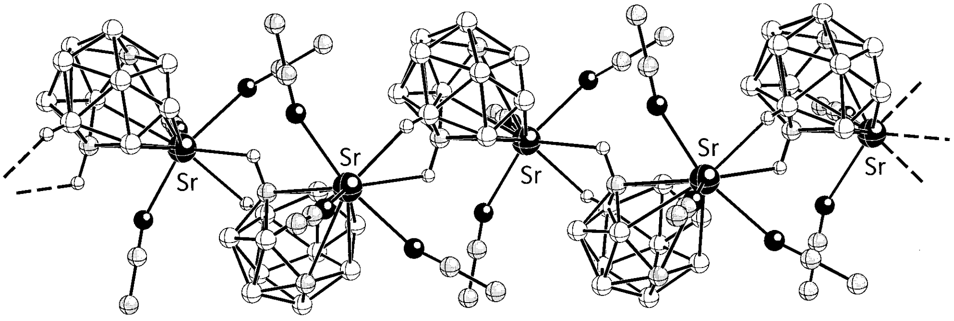

Fig. 20. A polymeric chain of $\{closo\text{-}(MeCN)_3\text{-}1,2,4\text{-}SrC_2B_{10}H_{12}\}_n$ [73], in which the Sr is coordinated by the open face of the carbaborane, bridging H–C–Sr and H–B–Sr interactions and the acetonitrile ligands.

*4.3.1.2.* $\{closo\text{-}(MeCN)_3\text{-}1,2,4\text{-}SrC_2B_{10}H_{12}\}_n$. The reaction of $Na_2[nido\text{-}7,9\text{-}C_2B_{10}H_{12}]$ with $SrI_2$ in THF at r.t. leads to the THF-solvated $(thf)_3\text{-}1,2,4\text{-}SrC_2B_{10}H_{12}$; recrystallization from $MeCN–Et_2O$ displaces the coordinated thf and produces a coordination polymer (Method D) (Fig. 20) [73]. Two similar, but crystallographically independent, spiral chains are found in the lattice. Each strontium atom is coordinated by three acetonitrile ligands, the open face ($\eta^6$) of the carbaborane ligand, and by C–H–Sr and C–H–Sr bridges from an adjacent cage. The Sr–B distances range from 2.87 to 3.08 Å, so the Sr–C contacts of 3.00(1) and 3.18(1) Å are not significantly different (the 3.00 Å Sr–C separation involves the carbon with the bridging hydrogen). It is curious that an C–H–Sr bridging interaction is present at all, as the more basic B–H bonds would be expected to be more attractive to the $Sr^{2+}$ center. In any case, the Sr···H–C and Sr···H–B distances are effectively the same at 2.62(9) and 2.56(9) Å, respectively.

### *4.3.2. Lewis acid–base adducts*

*4.3.2.1.* $Ca(C_5Me_5)_2(Me_3SiC{\equiv}C–C{\equiv}CSiMe_3)$. Bis(pentamethylcyclopentadienyl)-calcium, $Ca(C_5Me_5)_2$, reacts with 1,4-bis(trimethylsilyl)-1,3-butadiyne, $Me_3SiC{\equiv}C–C{\equiv}CSiMe_3$ (BTMSBD), in toluene to yield an orange-yellow 1:1 adduct (Method K) (Fig. 21). The $^1H$-NMR spectrum of the complex contains resonances for the $C_5Me_5$ ring and the diyne that are only slightly shifted from the values in the parent molecules, and addition of extra BTMSBD generates an averaged set of resonances for the methyne carbons, indicating that the free and complexed diyne are in fast exchange. The diyne is readily displaced by ethers and amines. Crystals of $Ca(C_5Me_5)_2(Me_3SiC{\equiv}C–C{\equiv}CSiMe_3)$ grown from hexane contain two independent molecules in the asymmetric unit. In one, the calcium is symmetrically associated with the center methyne carbons at distances of 2.991(5) and 3.024(5) Å; in the other, the diyne has slipped to one side of the ring centroid–Ca–ring centroid plane so that the center methynes are now at distances of 3.104(5) and 2.878(5) Å. The structural data are consistent with the solution NMR data in suggesting that the

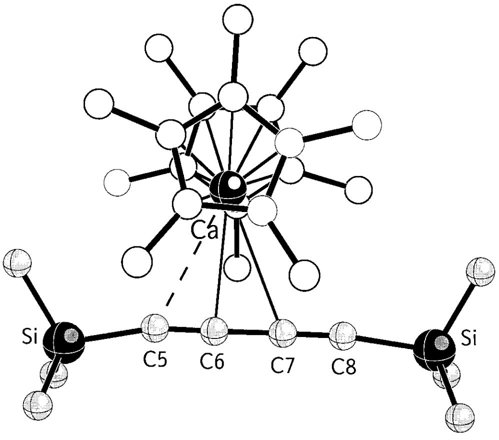

Fig. 21. One of the two crystallographically independent molecules of $Ca(C_5Me_5)_2(Me_3SiC{\equiv}C{-}C{\equiv}CSiMe_3)$ [50]; the Ca–C8 separation of 3.75 Å is clearly non-bonding; the energetic significance of the Ca–C5 separation (3.17 Å) is less certain.

Ca–diyne interaction is weak and flexible. The Ca–center methyne distances are considerably longer (by 0.24–0.46 Å) than the average Ca–$C_5Me_5$ distances, but the Ca–C(diyne) contact of 3.104 Å is paralleled by a long Ca–($\eta^1$-Cp) interaction at 3.100(2) Å in the structure of $CaCp_2$ [9]. A related yellow complex has been prepared from $Ca(C_5Me_5)_2$ and 2,4-hexadiyne [74].

*4.3.2.2. $Ae(C_5Me_5)_2(1,3,4,5\text{-}Me_4\text{-}C_3N_2)$ (Ae = Ca, Sr, Ba).* One equivalent of the stable carbene 1,3,4,5-tetramethylimidazol-2-ylidene reacts with the solvated metallocenes $Ca(C_5Me_5)_2(OEt_2)$, $Sr(C_5Me_5)_2(OEt_2)$, and $Ba(C_5Me_5)_2(thf)_2$ to displace the ethers and generate the $Ae(C_5Me_5)_2(1,3,4,5\text{-}Me_4\text{-}C_3N_2)$ adducts (Method K) [75]. The calcium and barium species have been structurally characterized, and display classic bent metallocene geometries with the carbene occupying the wedge between the rings. In the calcium complex (Fig. 22), the Ca–C(carbene) distance is 2.562(2)

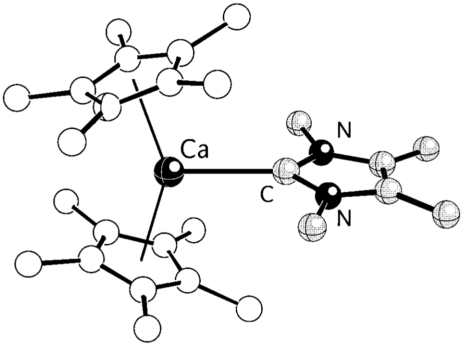

Fig. 22. Structure of the monomeric carbene adduct $Ca(C_5Me_5)_2(1,3,4,5\text{-}Me_4\text{-}C_3N_2)$ [75].

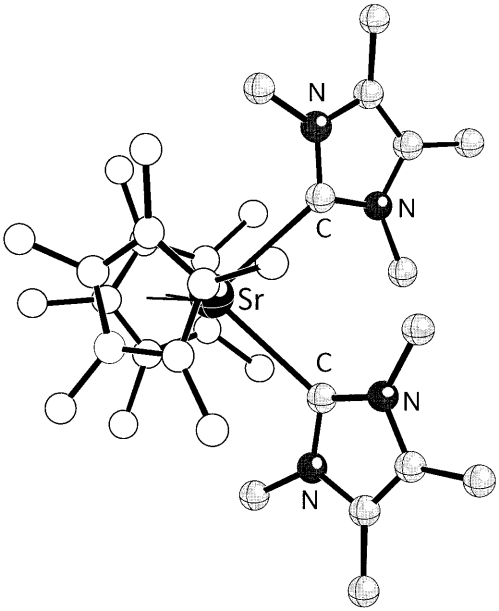

Fig. 23. Structure of the monomeric bis(carbene) adduct $Sr(C_5Me_5)_2(1,3,4,5\text{-}Me_4\text{-}C_3N_2)_2$ [75].

Å; it is 2.951(3) Å in the barium analogue. The 0.39 Å change is slightly greater than the 0.32 Å difference between the radii of seven-coordinate $Ca^{2+}$ and $Ba^{2+}$ [36]. In both complexes, the Ae–C(carbene) distance is shorter than the Ae–C($C_5Me_5$) separation, although the difference is slight in the barium compound (0.036 Å). In the calcium complex, the Ca–carbene vector lies in the plane of the imidazole ring, but in the barium, the ring is slightly tipped relative to the Ba–carbene vector. In the free carbene, the C–N–C angle is 101.5(1)° [76]; this value remains essentially unchanged in the complexes (i.e. 101.5(3)° (Ca) and 101.8(3)° (Ba)).

*4.3.2.3. $Ae(C_5Me_5)_2(1,3,4,5\text{-}Me_4\text{–}C_3N_2)_2$ (Ae = Sr, Ba).* Two equivalents of 1,3,4,5-tetramethylimidazol-2-ylidene react with $Sr(C_5Me_5)_2(OEt_2)$ and $Ba(C_5Me_5)_2(thf)_2$ to displace the ethers and generate the $Ae(C_5Me_5)_2(1,3,4,5\text{-}Me_4\text{–}C_3N_2)_2$ adducts (Method K) [75]. The strontium complex has been crystallographically characterized (Fig. 23), and the two ring centroids and the *ipso* carbon atoms of the carbene ligands define a distorted tetrahedron (twist between tetrahedral edges = 76.8°). The carbenes are at a similar distance from the metal (Sr–C(carbene) distances of 2.868(5) and 2.854(5) Å; $C\text{–}Sr\text{–}C' = 86.4(1)°$). As with the mono(carbene) species, the geometries of the coordinated carbenes are nearly undistorted from that of the free ligand (internal valence angles of 102.2(4) and 101.1(4)°) [76].

*4.3.2.4. $\{Ca(C_5Me_5)_2(\mu\text{-}CH_3)_2Al(CH_3)(thf)\}_2$.* This heterobimetallic complex is isolated from the reaction between $Ca(C_5Me_5)_2(thf)_2$ and $AlMe_3$ (Method K) [33]. The complex crystallizes as a centrosymmetric dimer that consists of two $Ca(C_5Me_5)_2$ units linked by bridging $Me_3Al(thf)$ groups, thereby generating an eight-membered

$[Ca–C(H_3)–Al–C(H_3)]_2$ ring (Fig. 24). Two of the methyl groups of each $Me_3Al(thf)$ moiety bridge the calcium centers ($Ca\cdots C(H_3) = 2.948(7)$, 2.999(7) Å); the third group remains terminal. Adduct formation at an Al center is known to enhance the carbanionic character of alkyl groups in $AlR_3$ species [77]. It is apparently this property that allows $AlMe_3$ to display bifunctional behavior toward $Ca(C_5Me_5)_2(thf)_2$, first as a Lewis acid (in extracting the thf from the calcium center) and secondly as a neutral base (interacting through the methyl groups of the thf adduct).

Unlike the behavior observed with $Ca(C_5Me_5)_2(thf)_2$, $CaCp_2(thf)_2$ completely transfers its coordinated thf to $AlMe_3$, and forms polymeric $\{CaCp_2\}_x$ [33]. Such oligomerization is not possible for base-free $Ca(C_5Me_5)_2$.

*4.3.2.5. Ba[(3,5-dimethylpyrazol-1-yl)₃Ge]₂(dioxane)₁/₂.* The poly(pyrazolyl) complex Ba(3,5-dimethylpyrazol-1-yl)$_2$ is formed from the reaction of barium metal and 3,5-dimethylpyrazole in refluxing THF (Method A). Subsequent reaction of the barium complex with $GeCl_2$·dioxane in THF produces Ba[(3,5-dimethylpyrazol-1-yl)$_3$Ge]$_2$(dioxane)$_{1/2}$ (Method K) [78]. Four of the anionic ligands are coordinated via their nitrogen atoms in a σ fashion (av Ba–N 2.80(3) Å), but two of the pyrazolyl groups are turned so that they are bound side-on to the barium (Fig. 25). There is a large spread in the ring–barium contact distances; the Ba–N lengths (av Ba–N5/N11 = 2.967 Å; Ba–N6/N12 = 2.927 Å) are longer than the σ-coordinated nitrogens, and the Ba–C distances are even longer (av Ba–C12/C27 = 3.393 Å; Ba–C14/C29 = 3.275 Å). The distances to the remaining carbon in each ring are > 3.5 Å, and should be considered non-bonding. The energetic significance of the long-range Ba–C interactions is difficult to assess, but it is worth noting that both side-on coordinated pyrazolyl rings are located *cis* with respect to the barium, even though a *trans* arrangement would minimize steric interactions.

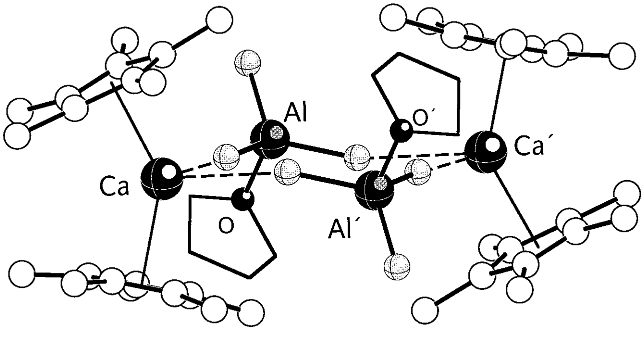

Fig. 24. Structure of the methyl-bridged dimer, $[(C_5Me_5)_2Ca(\mu\text{-}CH_3)_2Al(CH_3)(thf)]_2$. [33].

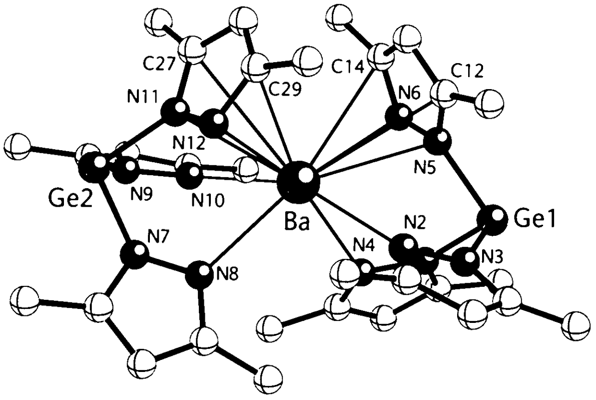

Fig. 25. Structure of the dimeric complex $Ba[(3,5\text{-dimethylpyrazol-1-yl})_3Ge]_2(\text{dioxane})_{1/2}$ [78].

## 5. Bonding in heavy Group 2 organometallic complexes

The highly electropositive nature of calcium, strontium, and barium generates metal–ligand interactions that are largely ionic, and the available structural information on Group 2 complexes reflects this. In classically ionic compounds, metal–ligand distances should be close to the sum of metal and ligand radii (i.e. $M\text{–}L = r_+ + r_-$). An analysis of cyclopentadienyl-containing organoalkaline-earth compounds supports this expectation; i.e. an accurate estimate of metal–cyclopentadienyl distances is provided by the sum of the coordination-adjusted value of the Shannon ionic radii [36] and the ‘van der Waals’ radius of the cyclopentadienyl ring (ca. 1.60 Å) [70]. This approach is related to that used by Raymond for (primarily trivalent) cyclopentadienyl lanthanide complexes [79], whose metal–cyclopentadienyl bonding is also mainly ionic. No comparable survey for non-cyclopentadienyl organoalkaline-earth complexes has been published, but there is little reason to think that similarly additive distances would not be found.

Lacking metal valence orbitals to influence the orientation of ligands, $AeL_2$ compounds would normally have linear geometries, as this arrangement serves to minimize intramolecular steric interactions. However, it has long been known that the Ae dihalides ($AeF_2$ (Ae = Ca, Sr, Ba); $AeCl_2$ (Ae = Sr, Ba); $BaI_2$), are bent in the gas phase [80,81] and in noble gas matrices [82]. In addition, the unsolvated dialkyl compound $Ca[C(SiMe_3)_3]_2$ is nonlinear [40], and with the exception of the sterically congested complex $Ba[C_5(^iPr)_5]_2$,[18], the metallocenes $Cp'_2Ae$ (and related divalent organolanthanide species [83,84]) possess non-parallel cyclopentadienyl rings.

It is possible to reconcile an electrostatically-based bonding scheme for $AeX_2$ compounds with their nonlinear structures by invoking ‘reverse polarization’ (core polarization) of the metal cation by the ligands [85–87], and a similar explanation has been suggested for organometallic derivatives [52,88]. The bending is understood as a consequence of charge-induced dipole interactions on the metal center, which favor non-linear structures. A related interpretation of the bending involves an analysis of Laplacian of the electron density in the core metal electrons [89,90]. The presence of appropriate ligands induces localization of electron pair density, and $AeX_2$ molecules are thus bent owing to a tetrahedrally distorted $Ae^{2+}$ core. A VSEPR-inspired approach can then be used to describe the bonding. This analysis makes correct predictions about the ordering of the bending for the dihalides (i.e. $Ca < Sr < Ba$; $F < Cl < Br < I$), although the extent of the polarizability of the metal cations' noble-gas cores has been debated [91,92].

It should be noted that explanations based on polarization use the language of electrostatics to describe a phenomenon that could also be couched in molecular orbital terms; i.e. an ion is 'polarizable' to the extent that it has low-lying vacant orbitals (in the case of the alkaline-earth elements, $(n-1)$ d or n s orbitals). Interaction of the anionic ligands with a 'polarizable' metal center is equivalent to interaction with these vacant orbitals. This is especially relevant for the Group 2 elements, which are electronic neighbors of the transition metals. It has been pointed out, for example, that the 3d orbitals in calcium, although formally vacant, must be considered part of the metal's valence space in order to obtain accurate results from molecular orbital computations [93]. Calculations on wide range of small molecules, including $AeH_2$, $AeLi_2$, $Ae(BeH)_2$, $Ae(BH_2)_2$, $Ae(CH_3)_2$, $Ae(NH_2)_2$, $Ae(OH)_2$, and $AeX_2$ ($Ae = Ca$, Sr, Ba) predict that they should always be bent when the metal is strontium or barium; whether calcium complexes are expected to be bent depends critically on the level of theory employed [92,94–99]. The energies involved in bending are sometimes substantial (e.g. the linearization energy of $Ba(NH_2)_2$ is placed at ca. 28 kJ $mol^{-1}$ [95]). Experimental confirmation of the bending angles in most of these small species is not available, however.

## 5.1. Computational considerations

To date, there have been comparatively few computational studies of the heavy alkaline-earth organometallics, and most of these have focused on the metallocenes. Calculations intended to reproduce the geometries of heavy Group 2 organometallic species have had mixed success, and underscore the need for very high quality methods and large basis sets to replicate observed geometries. For example, Hartree–Fock calculations have indicated that $CaCp_2$ and $SrCp_2$ should be linear (using all-electron basis sets) [100] or 'quasilinear' (using quasirelativistic pseudopotential basis sets) [101], contrary to the experimentally determined gas-phase and solid state structures of the alkylated derivatives [51,52,100,102,103]. $BaCp_2$, however, has been predicted to be bent (147°), with a linearization energy of 1.5 kJ $mol^{-1}$ (HF/MP2, quasirelativistic pseudopotentials) [101]. The latter figure is close to that estimated necessary to bend the decamethylmetallocenes by 20° in the gas phase (2 to 3.5 kJ $mol^{-1}$) [100,102]. More recent calculations using all-electron basis sets and either HF/MP2 or density functional theory methods have identified bent minima for all three $Cp_2Ae$ metallocenes [90,104,105].

The only other compounds falling under the scope of this review that have been studied computationally are the methyl derivatives, $Ae(CH_3)_2$ and $Ca(CH_3)H$. As with the metallocenes, predictions about whether the dimethyl compounds should be linear or bent vary with the method and basis sets used, but recent calculations favor bent structures with all three metals (Table 2). A matrix isolation study identified $Ca(CH_3)H$ in the cocondensate from calcium atoms and methane with argon at 10 K [106]. The assignment of the IR spectrum (409/419 $cm^{-1}$ to $\rho(CH_3)$ and 1245/1254/1263 $cm^{-1}$ to $\nu$(Ca–H) modes) was based on comparisons to related magnesium and beryllium species. DFT calculations suggest that these assignments are reasonable; $Ca(CH_3)H$ is predicted to be bent (BLYP/6-311G(df,p); C–Ca–H = 125.9°), with three $\rho(CH_3)$ at 397, 406, and 422 $cm^{-1}$ and $\nu$(Ca–H) at 1250 $cm^{-1}$ [107].

The experimental and theoretical studies completed to date agree that Group 2 organometallic compounds are highly polar, 'floppy' systems, with nearly flat potential energy bending curves. Owing to this, covalent or van der Waals effects [108], even if they involve only small energies, may have a disproportionally large influence on geometries. As noted in a study of the structure of $CaF_2$ [99], calculations involving the heavy Group 2 elements must employ large, flexible basis sets (e.g. usually of triple zeta quality, with multiple d or even f functions on the metals) and some accounting must be made for electron correlation in order to insure that reliable results are produced. The increasingly widespread use of computationally efficient density functional theory methods, which provide for such effects [109–111], may encourage the exploration of larger systems. It should also be emphasized that molecular orbital calculations that successfully reproduce bent geometries and explicitly include valence d orbitals in the basis sets do not prove that the 'reverse polarization' approach to interpreting the bonding in these compounds is invalid, as the d-orbitals that are used are usually highly contracted, and in practice act as polarizing functions for the metal cores stress.

## 6. Applications

Even though the alkyl halide derivatives of the heavier alkaline-earth metals have not yet achieved the widespread applicability in organic chemistry as have Grignard reagents (Section 1), it is interesting to note that new synthetic applications for compounds of the heavier metals are appearing that differ in useful ways from those provided by organomagnesium compounds. As many of these involve non-cyclopentadienyl complexes, we note those that have been reported in the last 10 years. Earlier work is described in several reviews [21,23].

Yamamoto has demonstrated in a series of papers that allylbarium compounds typically react at the least hindered (usually α-) position of the allyl moiety, contrary to the behavior normally observed with other organometallic allyls. For example, solutions containing allylbarium compounds have been found to be regio- and stereospecific allylation agents for carbonyl compounds [16,112]. Stereochemically homogeneous (*E*)- and (*Z*)-β,γ-unsaturated carboxylic acids are prepared in good yields by highly α-selective carboxylation of allylic barium reagents with carbon dioxide (Eq. (1)). It is possible that the long Ba–C bonds in the allylbarium

Table 2
Optimized geometries of heavy Group 2 dimethyl complexes, $Ae(CH_3)_2$

| Complex | Ae–C distance (Å) | C–Ae–C′(°) | Linearization energy (kJ $mol^{-1}$) | Method/basis set | Ref. |
|---|---|---|---|---|---|
| $Ca(CH_3)_2$ | 2.487 | 180 | Quasilinear | HF/quasirelativisitic pseudopotential | [95] |
| $Ca(CH_3)_2$ | 2.452 (2.458 if linear) | 157.9 | 1.7 | HF/MP2/all-electron | [89] |
| $Ca(CH_3)_2$ | 2.408 (2.437 if linear) | 135.9 | 0.9 | DFT/B3PW91/6-311G(d) | [107] |
| $Sr(CH_3)_2$ | 2.621 (2.673 if linear) | 130.6 | 7.4 | HF/quasirelativisitic pseudopotential | [95] |
| $Ba(CH_3)_2$ | 2.757 (2.937 if linear) | 115.9 | 33 | HF/quasirelativisitic pseudopotential | [95] |

reagents prevent the generation of six-membered cyclic transition structures that could react at the γ-carbons.

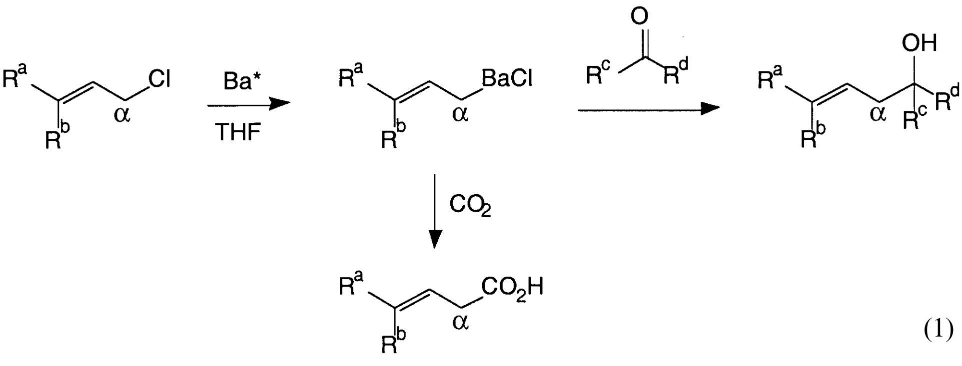

(1)

Selective 1,4-Michael addition reactions with α,β-unsaturated cycloalkanones are also achieved using allylbarium reagents (Eq. (2)).

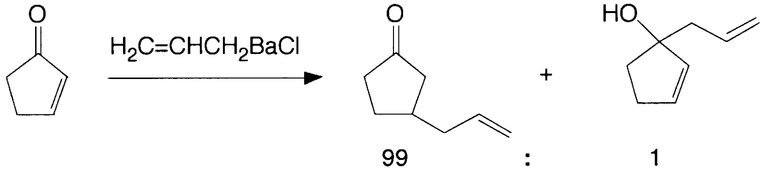

(2)

Comparable selectivities cannot be obtained with Grignard or organolithium reagents. Regioselective coupling of allylbarium species with epoxides also displays high α selectivity (Eq. (3)) [113],

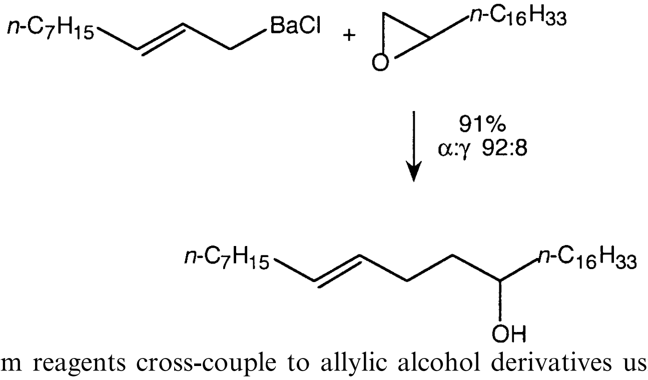

(3)

and allylbarium reagents cross-couple to allylic alcohol derivatives using bis(2,2,2-trifluoroethyl)phosphate as a leaving group to yield 1,5-dienes with high α,α′-selectivity [114]. Under similar conditions, Grignard reagents produce α:γ coupled products.

An unusual temperature dependence on the regioselective behavior of an allylbarium species has been demonstrated in asymmetric allylation with the optically active imine SAMP-hydrazone [SAMP = (*S*)-( − )-1-amino-2-methoxymethylpyrrolidine] (Eq. (4)).[115] Its reaction with prenylbarium chloride at 0°C produced an α-allylated hydrazine in 60% diastereotopic excess, but at − 78°C, the γ-adduct was generated with 98% diastereotopic excess.

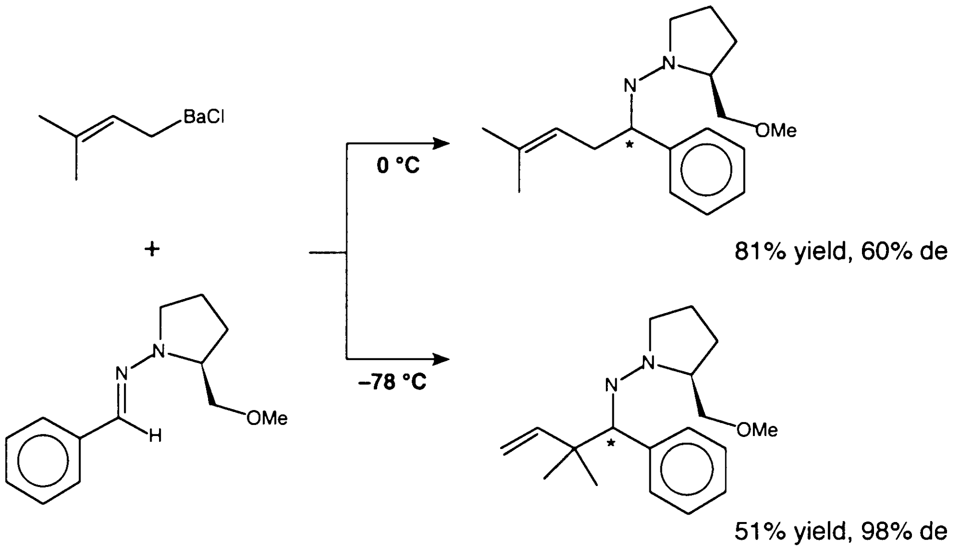

(4)

The temperature dependence of the α/γ ratio may reflect competition between a kinetically favored γ-adduct at low temperature and a thermodynamically preferred α-form at higher temperatures.

Highly reactive metal powders formed from the reduction of $CaI_2$ with lithium biphenylide react with halogenated polystyrenes to form thermally stable organocalcium reagents [15]. These in turn react with various electrophiles (e.g. $CO_2$, $ClSiMe_3$, cyclohexanone, 1,2-epoxybutane) to yield functionalized polymers (Eq. (5)).

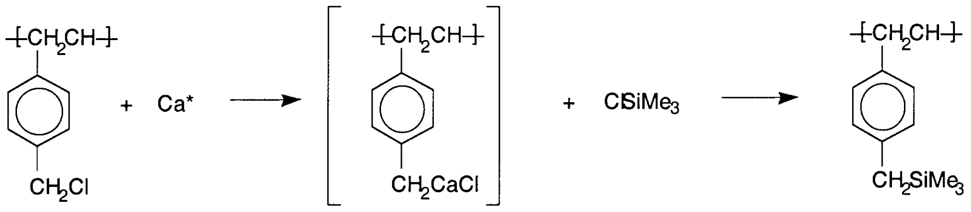

(5)

The halogenated polymers undergo transmetallation with CuCN to produce calcium cuprates, which generate ketone-containing polymers from acid halides, and undergo 1,4-addition with α,β-unsaturated ketones. The calcium-derived reagents will also react with functionalized polystyrenes containing a halogen (e.g. PS–$COC_6H_4$(*p*-Cl)) to yield bifunctionalized polymers.

A novel route to aryl-nitrogen compounds involving an organocalcium system that has no direct counterpart in Grignard chemistry was first reported over 40 years ago [116] and has been reinvestigated [117]. The reaction of phenylcalcium iodide with nitrous oxide in diethyl ether yields a mixture of products presumably arising from insertion of $N_2O$ into the phenyl–calcium bond, including azobenzene (15%), benzidene, and *N*-phenylbenzidene. Subsequent examination of this reaction found that the distribution and yield of products are strongly dependent on the solvent used; the yield of azobenzene, for example, rises to 61% in dimethoxyethane. The reaction also occurs with diphenylcalcium itself, which could form from the Schlenk redistribution of phenylcalcium iodide (i.e. Eq. (6)).

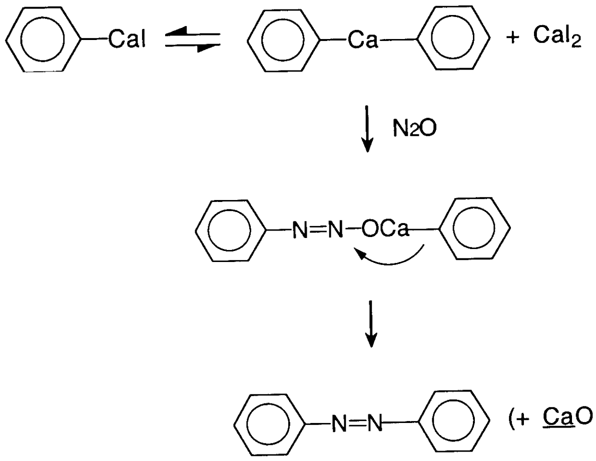

(6)

The reaction of calcium, strontium, or barium vapor with cyclooctatetraene and THF at −196°C yields complexes of the form Ae(COT)(thf)$_n$; the coordinated thf is removed on heating at 60°C [118]. The base-free substances form adducts with pyridine (Ae(COT)(pyridine)$_n$), and abstract the chlorine from benzyl chloride to produce the Wurtz-coupled product $(PhCH_2)_2$. With trityl chloride in THF, in contrast, they serve as a source of the metal, and generate the trityl metal halides, $Ae(CPh_3)Cl(thf)_n$.

The Ae(COT) species react with $CH_2Cl_2$ to produce bicyclo[6.1.0]nonatriene (Eq. (7)), and with $Ph_2C(C_5H_4N\text{-}2)PCl_2$ to yield a novel thermally stable phosphacyclopropane. In these last two cases, Ae(COT) has served as a source of the $[COT]^{2-}$ anion.

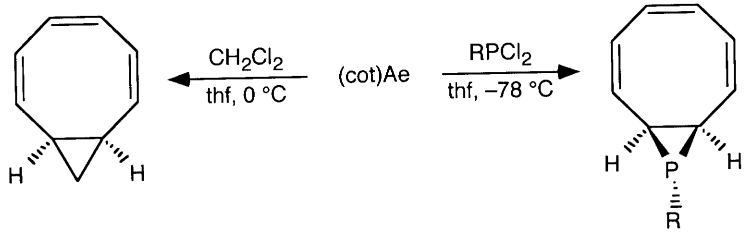

(7)

## 7. Conclusions

Continuing a century-long history of development, progress in heavy Group 2 organometallic chemistry has been greatly accelerated in the past two decades. The recognition that compounds of the heavier alkaline-earth metals share similarities in structure and reactivity with those of the lanthanide elements has contributed to this growth. A contributing factor of equal importance has been the use in synthesis of sterically bulky ligands, which has markedly increased the solubility and kinetic stability of many alkaline-earth compounds, and has made possible the isolation and detailed characterization of new non-cyclopentadienyl based compounds. Numerous challenges remain in extending the chemistry of these compounds, and there are intriguing questions about their bonding and patterns of reactivity that need to be addressed. Especially interesting will be determining the extent to which ligand size can be tuned, so that compounds can be synthesized that are kinetically stable enough to be used in a controlled manner, and yet are not so heavily decorated that their reactivity becomes too limited. Such control is central to expanding the role of calcium, strontium, and barium compounds in material science and organic synthesis.

## Acknowledgements

Acknowledgment for support of research from my laboratory is made to the National Science Foundation.

## References

[1] E. Beckman, Chem. Ber. 38 (1905) 904.
[2] H. Gilman, F. Schulze, J. Am. Chem. Soc. 48 (1926) 2463.
[3] H. Gilman, A.H. Haubein, G. O'Donnell, L. Woods, J. Am. Chem. Soc. 65 (1943) 268.
[4] P.L. Pauson, T.J. Kealy, Nature 168 (1951) 1039.
[5] E.O. Fischer, H.P. Hofmann, Chem. Ber. 92 (1959) 482.
[6] E. Weiss, E.O. Fischer, Z. Anorg. Allg. Chem. 278 (1955) 219.
[7] K. Ziegler, H. Froitzheim-Kühlhorn, H. Hafner, Chem. Ber. 89 (1956) 434.
[8] E.O. Fischer, G. Stölzle, Chem. Ber. 94 (1961) 2187.
[9] R. Zerger, G. Stucky, J. Organomet. Chem. 80 (1974) 7.
[10] J.V. Mantese, A.B. Catalan, A.H. Hamdi, A.L. Micheli, Appl. Phys. Lett. 52 (1988) 1741.
[11] L.G. Hubert-Pfalzgraf, Nouv. J. Chem. 11 (1987) 663.
[12] D.C. Bradley, Philos. Trans. R. Soc. London A 330 (1990) 167.
[13] M.J. Benac, A.H. Cowley, R.A. Jones, A.F. Tasch Jr., Chem. Mater. 1 (1989) 289.
[14] T.C. Wu, H. Xiong, R.D. Rieke, J. Org. Chem. 55 (1990) 5045.
[15] R.A. O'Brien, T. Chen, R.D. Rieke, J. Org. Chem. 57 (1992) 2667.
[16] A. Yanagisawa, S. Habaue, K. Yasue, H. Yamamoto, J. Am. Chem. Soc. 116 (1994) 6130.

[17] A. Yanagisawa, K. Ogasawara, K. Yasue, H. Yamamoto, J. Chem. Soc. Chem. Commun. (1996) 367.
[18] H. Sitzmann, T. Dezember, M. Ruck, Angew. Chem. Int. Ed. Engl. 37 (1998) 3114.
[19] S.C. Sockwell, T.P. Hanusa, J.C. Huffman, J. Am. Chem. Soc. 114 (1992) 3393.
[20] M.J. Harvey, T.P. Hanusa, Organometallics 19 (2000) 1556.
[21] W.E. Lindsell, in: G. Wilkinson, F.G.A. Stone, E. Abel (Eds.), Comprehensive Organometallic Chemistry, Pergamon, Oxford, 1982, p. 223.
[22] W.E. Lindsell, in: G. Wilkinson, F.G.A. Stone, E. Abel (Eds.), Comprehensive Organometallic Chemistry II, Pergamon, Oxford, 1995, p. 107.
[23] T.P. Hanusa, Polyhedron 9 (1990) 1345.
[24] T.P. Hanusa, Chem. Rev. 93 (1993) 1023.
[25] D.J. Burkey, T.P. Hanusa, Comments Inorg. Chem. 17 (1995) 41.
[26] M.L. Hays, T.P. Hanusa, Adv. Organomet. Chem. 40 (1996) 117.
[27] P. Jutzi, N. Burford, Chem. Rev. 99 (1999) 969.
[28] J.S. Overby, T.P. Hanusa, Organometallics 15 (1996) 2205.
[29] G. Mösges, F. Hampel, P.v.R. Schleyer, Organometallics 11 (1992) 1769.
[30] S. Harder, M. Lutz, A.W.G. Straub, Organometallics 16 (1997) 107.
[31] N. Leyser, K. Katrin Schmidt, H.-H. Brintzinger, Organometallics 17 (1998) 2155.
[32] D.J. Burkey, T.P. Hanusa, Organometallics 15 (1996) 4971.
[33] P.S. Tanner, R.A. Williams, T.P. Hanusa, Inorg. Chem. 32 (1993) 2234.
[34] W.-T. Chan, I.P. Hamilton, Chem. Phys. Lett. 297 (1998) 217.
[35] P.F. Bernath, Adv. Photochem. 23 (1997) 1.
[36] R.D. Shannon, Acta Crystallogr. Sect A. 32 (1976) 751.
[37] A.L. Allred, E.G. Rochow, J. Inorg. Nucl. Chem. 5 (1958) 264.
[38] W.J. Evans, Adv. Organomet. Chem. 24 (1985) 131.
[39] W.J. Evans, Polyhedron 6 (1987) 803.
[40] C. Eaborn, S.A. Hawkes, P.B. Hitchcock, J.D. Smith, J. Chem. Soc. Chem. Commun. (1997) 1961.
[41] F.G.N. Cloke, P.B. Hitchcock, M.F. Lappert, G.A. Lawless, B. Royo, J. Chem. Soc. Chem. Commun. (1991) 724.
[42] K. Mochida, T. Yamanishi, J. Organomet. Chem. 332 (1987) 247.
[43] K. Mochida, H. Takeuchi, Y. Hiraga, H. Ogawa, Organometallics 6 (1987) 2293.
[44] M.J. McCormick, K.B. Moon, S.R. Jones, T.P. Hanusa, J. Chem. Soc. Chem. Commun. (1990) 778.
[45] B.A. Vaartstra, J.C. Huffman, W.E. Streib, K.G. Caulton, Inorg. Chem. 30 (1991) 121.
[46] M. Westerhausen, Inorg. Chem. 30 (1991) 96.
[47] M. Westerhausen, Coord. Chem. Rev. 176 (1998) 157.
[48] S.A. Kinsley, A. Streitwieser Jr., A. Zalkin, Organometallics 4 (1985) 52.
[49] Lappert has reported a similar reaction between $Ae(OSO_2C_6H_4Me\text{-}4)_2$ (Ae = Ca, Sr, Ba) and $LiCH(SiMe_3)_2$ in THF to yield $LiAe(OSO_2C_6H_4Me\text{-}4)_2[CH(SiMe_3)_2]$ (thf) (A.D. Frankland, M.F. Lappert, J. Chem. Soc. Dalton Trans. 22 (1996) 4151).
[50] R.A. Williams, T.P. Hanusa, J.C. Huffman, J. Am. Chem. Soc. 112 (1990) 2454.
[51] R.A. Andersen, J.M. Boncella, C.J. Burns, R. Blom, A. Haaland, H.V. Volden, J. Organomet. Chem. 312 (1986) C49.
[52] R.A. Williams, T.P. Hanusa, J.C. Huffman, Organometallics 9 (1990) 1128.
[53] M.J. Harvey, T.P. Hanusa, M. Pink, J. Chem. Soc. Chem. Commun. (2000) 489.
[54] D.C. Green, U. Englich, K. Ruhlandt-Senge, Angew. Chem. Int. Ed. Engl. 38 (1999) 354.
[55] M. Westerhausen, M.H. Digeser, H. Noth, T. Seifert, A. Pfitzner, J. Am. Chem. Soc. 120 (1998) 6722.
[56] S. Searles, Y. Li, B. Nassim, M.-T.R. Lopes, P.T. Tran, P. Crabbe, J. Chem. Soc. Perkin Trans. 1 (1984) 747.
[57] M.J. Harvey, T.P. Hanusa, V.G. Young Jr., Angew. Chem. Int. Ed. Engl. 38 (1999) 217.
[58] N.v.E. Hommes, M. Bühl, P.v.R. Schleyer, Y.-D. Wu, J. Organomet. Chem. 409 (1991) 307.
[59] R. Goddard, C. Krüger, F. Mark, R. Stansfield, X. Zhang, Organometallics 4 (1985) 285.

[60] K. Mashima, H. Sugiyama, N. Kanehisa, Y. Kai, H. Yasuda, A. Nakamura, J. Am. Chem. Soc 116 (1994) 6977.

[61] J.S. Overby, T.P. Hanusa, Angew. Chem. Int. Ed. Engl. 33 (1994) 2191.

[62] H. Yasuda, Y. Ohnuma, A. Nakamura, Y. Kai, N. Yasuoka, N. Kasai, Bull. Chem. Soc. Jpn. 53 (1980) 1101.

[63] M.J. McCormick, S.C. Sockwell, C.E.H. Davies, T.P. Hanusa, J.C. Huffman, Organometallics 8 (1989) 2044.

[64] P. Jutzi, W. Leffers, G. Müller, B. Huber, Chem. Ber. 122 (1989) 879.

[65] L.M. Engelhardt, P.C. Junk, C.L. Raston, A.H. White, J. Chem. Soc. Chem. Commun. (1988) 1500.

[66] R.D. Ernst, C.F. Campana, D.R. Wilson, J.Z. Liu, Inorg. Chem. 23 (1984) 2732.

[67] S. Harder, M. Lutz, Organometallics 16 (1997) 225.

[68] M.G. Gardiner, C.L. Raston, H. Viebrock, J. Chem. Soc. Chem. Commun. (1996) 1795.

[69] M. Westerhausen, M.H. Digeser, C. Gückel, H. Noth, J. Knizek, W. Ponikwar, Organometallics 18 (1999) 2491.

[70] S.C. Sockwell, T.P. Hanusa, Inorg. Chem. 29 (1990) 76.

[71] W. Clegg, S.J. Coles, E.K. Cope, F.S. Mair, Angew. Chem. Int. Ed. Engl. 37 (1998) 796.

[72] R. Khattar, C.B. Knobler, M.F. Hawthorne, J. Am. Chem. Soc. 112 (1990) 4962.

[73] R. Khattar, C.B. Knobler, M.F. Hawthorne, Inorg. Chem. 29 (1990) 2191.

[74] R.A. Williams, Aug. 1991.

[75] A.J. Arduengo, F. Davidson, R. Krafczyk, W.J. Marshall, M. Tamm, Organometallics 17 (1998) 3375.

[76] A.J. Arduengo, H.V.R. Dias, R.L. Harlow, M. Kline, J. Am. Chem. Soc. 114 (1992) 5530.

[77] C. Elschenbroich, A. Salzer, Organometallics: A Concise Introduction, VCH, New York, 1992, p. 85.

[78] A. Steiner, D. Stalke, Inorg. Chem. 34 (1995) 4846.

[79] K.N. Raymond, C.W. Eigenbrot, Acc. Chem. Res. 13 (1980) 276.

[80] L. Wharton, R.A. Berg, W. Klemperer, J. Chem. Phys. 39 (1963) 2023.

[81] V.V. Kasparov, Y.S. Ezhov, N.G. Rambidi, J. Struct. Chem. 20 (1979) 260.

[82] R. Sugarman, M. Wilson, P.A. Madden, Chem. Phys. Lett. 308 (1999) 509.

[83] W.J. Evans, L.A. Hughes, T.P. Hanusa, J. Am. Chem. Soc. 106 (1984) 4270.

[84] W.J. Evans, L.A. Hughes, T.P. Hanusa, R.J. Doedens, Organometallics 5 (1986) 1285.

[85] M. Guido, G. Gigli, J. Chem. Phys. 65 (1976) 1397.

[86] P.A. Madden, M. Wilson, Chem. Soc. Rev. 25 (1996) 339.

[87] R. Sugarman, M. Wilson, P.A. Madden, Chem. Phys. Lett. 308 (1999) 509.

[88] J.C. Green, D. Hohl, N. Rösch, Organometallics 6 (1987) 712.

[89] I. Bytheway, R.J. Gillespie, T.H. Tang, R.F.W. Bader, Inorg. Chem. 34 (1995) 2407.

[90] I. Bytheway, P.L.A. Popelier, R.J. Gillespie, Can. J. Chem. 74 (1996) 1059.

[91] L.s. von Szentpály, P. Schwerdtfeger, Chem. Phys. Lett. 170 (1990) 555.

[92] R.L. Dekock, M.A. Peterson, L.K. Timmer, E.J. Baerends, P. Vernooijs, Polyhedron 9 (1990) 1919.

[93] J.-P. Blaudeau, M.P. McGrath, L.A. Curtiss, L. Radom, J. Chem. Phys. 107 (1997) 5016.

[94] M. Kaupp, P.v.R. Schleyer, H. Stoll, H. Preuss, J. Am. Chem. Soc. 113 (1991) 6012.

[95] M. Kaupp, P.v.R. Schleyer, J. Am. Chem. Soc. 114 (1992) 491.

[96] M. Kaupp, P.v.R. Schleyer, H. Stoll, H. Preuss, J. Chem. Phys. 94 (1991) 1360.

[97] L. Seijo, Z. Barandiarán, S. Huzinaga, J. Chem. Phys. 113 (1991) 3762.

[98] D.M. Hassett, C.J. Marsden, J. Chem. Soc. Chem. Commun. (1990) 667.

[99] D.M. Hassett, C.J. Marsden, J. Mol. Struct. 346 (1995) 249.

[100] R. Blom, K. Faegri Jr., H.V. Volden, Organometallics 9 (1990) 373.

[101] M. Kaupp, P.v.R. Schleyer, M. Dolg, H. Stoll, J. Am. Chem. Soc. 114 (1992) 8202.

[102] R.A. Andersen, R. Blom, C.J. Burns, H.V. Volden, J. Chem. Soc. Chem. Commun. (1987) 786.

[103] R.A. Andersen, R. Blom, J.M. Boncella, C.J. Burns, H.V. Volden, Acta Chem. Scand. A41 (1987) 24.

[104] A.J. Bridgeman, J. Chem. Soc. Dalton. Trans. 17 (1997) 2887.

[105] V. Milman, M.H. Lee, J. Phys. Chem. (1996) 6093.
[106] T.M. Greene, D.V. Lanzisera, L. Andrews, A.J. Downs, J. Am. Chem. Soc. 120 (1998) 6097.
[107] J.D. Smith, T.P. Hanusa, manuscript in preparation.
[108] T.K. Hollis, J.K. Burdett, B. Bosnich, Organometallics 12 (1993) 3385.
[109] R.G. Parr, W. Yang, Density Functional Theory of Atoms and Molecules, Oxford University Press, Oxford, 1989.
[110] J.K. Labanowski, J.W. Andelm (Eds.), Density Functional Methods in Chemistry, Springer-Verlag, New York, 1991.
[111] T. Ziegler, Chem. Rev. 91 (1991) 651.
[112] A. Yanagisawa, S. Habaue, H. Yamamoto, J. Am. Chem. Soc. 113 (1991) 8955.
[113] K. Yasue, A. Yanagisawa, H. Yamamoto, Bull. Jpn. Chem. Soc. 70 (1997) 493.
[114] A. Yanagisawa, K. Yasue, H. Yamamoto, Synlett 9 (1996) 842.
[115] A. Yanagisawa, K. Ogasawara, K. Yasue, H. Yamamoto, J. Chem. Soc. Chem. Commun. (1996) 367.
[116] R. Meier, K. Rappold, Angew. Chem. 65 (1953) 560.
[117] M.L. Hays, T.P. Hanusa, Tetrahedron Lett. 36 (1995) 2435.
[118] D.S. Hutchings, P.C. Junk, W.C. Patalinghug, C.L. Raston, A.H. White, J. Chem. Soc. Chem. Commun. 15 (1989) 973.